The Empirical Influences of Tibetan Plateau Soil Moisture on South Asian Monsoon Onset

Dan Lou
Nanjing University of Information Science and Technology
Guojie Wang (gwang@nuist.edu.cn)
Nanjing University of Information Science and Technology
waheed ullah
Nanjing University of Information Science and Technology https://orcid.org/0000-0002-0626-0650
Zhiqiu Gao
Nanjing University of Information Science and Technology
Asher Samuel Bhatti
Nanjing University of Information Science and Technology
Daniel Fiifi Tawia Hagan
Nanjing University of Information Science and Technology
Tong Jiang
Nanjing University of Information Science and Technology
Buda Su
China Meteorological Administration
Chenxia Zhu
Nanjing University of Information Science and Technology

Research Article

Keywords: Tibet Plateau, Soil moisture, South Asian High, Energy fluxes, Monsoon onset

Posted Date: March 2nd, 2021

DOI: https://doi.org/10.21203/rs.3.rs-238667/v1

Abstract

The South Asian High (SAH) location and intensity are linked with the Tibetan Plateau (TP) and Yangtze River basin latent heating. The existing feedbacks of SAH variability is rarely linked with TP soil moisture regulated energy fluxes. In this study, remotely sensed soil moisture and global atmospheric reanalysis products are used to quantify the relationship between the TP spring (April, May, June) soil moisture with SAH and South Asian (SA) monsoon onset during 1988–2008. The diagnostic analysis infers that the SAH exhibits a significant correlation ($R \geq 0.90$) with TP spring soil moisture and monsoon onset indices ($R \geq -0.56 – -0.61$). During the early and late monsoon onset, a significant anomalous soil moisture regime influenced the surface energy fluxes, which affected the vertical diabatic heating profile. The diabatic heating profile affects the TP ascending motion and SAH intensity, which leads to regional monsoon circulation changes and onset. An asymmetric SAH movement in the upper troposphere appears before the early and late monsoon onset composites and drives the lower tropospheric westerlies/easterlies winds towards the continental SA. The wind shear and transition from prevailing easterlies into westerlies during the pre-onset, onset, and post-onset pentad results in strong/weak ascent in the Bay of Bengal and advances into continental regions. The onset- mechanism further suggested intensified/weaker westerlies/easterlies during early/late onset composites. The SAH intensity and movement are linked with TP soil moisture, which exhibits teleconnections with the regional circulation pattern. A detailed model experiment will be conducted to verify the influence of soil moisture as a driver of energy fluxes and SA monsoon onset.

1 Introduction

The Tibetan Plateau (TP) thermal and mechanical controls are known as regional climate drivers (Anmin et al. 2012; Wang et al. 2019a; Xie et al. 2020). The TP's elevated surface has relatively lower pressure and acts as a heat sink/source during cold/warm seasons (Anmin et al. 2012; Huang et al. 2018). The elevated topography receives an enormous amount of radiation during the spring and summer seasons, which is partly used as latent heat (LH), sensible heat (SH), and ground heat (GH) (Wu et al. 2012). These fluxes govern shallow cyclonic and deep anticyclonic circulations over TP during the summer (Anmin et al. 2012). In the troposphere, low/high-pressure systems are linked with such energy fluxes that result in wind ascent/descent, influencing the local and remote meteorological fields., e.g., precipitation and temperature (Wang et al. 2016a, a). The plateau heat fluxes influence the local microphysical precipitation (Wang et al. 2016b); and they also influence the Asian-Pacific oscillation, the Rossby wave, and the Hadley cell circulation (Anmin et al. 2012; Lu et al. 2017), as well as the Asian monsoon system (Duan et al. 2017; Wang et al. 2017a).

The TP thermal and mechanical forcing are studied with empirical approaches and coupled atmospheric-ocean general circulation models. Using a coupled atmosphere-ocean circulation model, Abe et al. (2013) found that TP's presence leads to strong air-sea interactions and, consequently, variable onset of SA monsoon. He et al. (2019) used a coupled general circulation model with multiple initializations and prescribed forcing's to study the TP influences. It was suggested that the combined thermal effects of TP

and Iranian Plateau (IP) could modify the tropospheric cyclonic circulation, transporting water vapors to continental SA. Using the Weather Research and Forecast (WRF) model, Wang et al. (2019b) found a significant negative relationship between southeastern TP thermal forcing and summer precipitation over Pakistan. Wu et al. (2012) found that the TP thermal controls over both components of the Asian Monsoon (SA and EASM) are significantly stronger than its mechanical forcing, whereas the EASM component of the Asian Monsoon is more sensitive to TP thermal profile than SA. Wang et al. (2017a) argued that the TP control both EASM and SA monsoon systems; without TP uplift, the SA monsoon will be much weaker than the present day, whereas the EASM will disappear.

Furthermore, the vertical profile of TP thermal heating influences the tropospheric anticyclonic patterns, known as South Asian High (SAH); and the SAH exhibits strong feedbacks with TP thermal heating (Zhang et al. 2016; Ge et al. 2019). The variability of TP thermal heating influences, the east/west transition of SAH and intensification of Western pacific subtropical high (WPSH), resulting in variability of monsoon precipitation (Wei et al. 2015; Wu et al. 2015; Zhang et al. 2016; Ge et al. 2019). The zonal movement of the SAH exhibits two distinct modes termed Tibetan plateau mode and Iranian plateau mode; altogether, these two modes influence the SA monsoon precipitation variability. The TP and Asian monsoon's thermal heating altogether modify the center and the meridional movement of the SAH, which affects the monsoon onset and precipitation (Ge et al. 2018).

There are mid-tropospheric circulations in the monsoon season, which transport the moisture contents from the Indian Ocean (Pathak et al. 2017b), due to the shifting in heat maxima from the southern hemisphere to the northern hemisphere (Xavier et al. 2007; Liu et al. 2012). Monsoon precipitation is linked with an abrupt change in mid-tropospheric circulation shear, resulting in 65–85% of the regional precipitation in SA (Naidu et al. 2017; Prabhu et al. 2017; Ullah et al. 2018a). The SA monsoon onset dates are defined based on multiple approaches, and they are mostly based on precipitation amount, air temperature, and humidity (Zhang et al. 2002; Stolbova et al. 2016) or the seasonal reversal of winds and temperature gradients (Wang and Fan 1999; Xavier et al. 2007). Several studies have found that the TP forcing's may lead to the early/delayed onset of SA monsoon (Wu and Zhang 1998; Park et al. 2012; Abe et al. 2013; He et al. 2019).

Studies of TP forcing's have indicated that the thermal process of a sensible-heat-driven air pump (SHAP) is dominant over the mechanical forcing (Wu et al. 2007, 2012). However, the land surface parameters, especially soil moisture, have not been explicitly studied in affecting the TP thermal conditions. Soil moisture anomalies can persist for months, affecting the albedo and thermal fluxes (Seneviratne et al. 2010), and thus they can influence the coupled interactions between the land, atmosphere, and oceans (Koster et al. 2016). Such soil moisture effects have been studied for the African monsoon (Berg et al. 2017), Indian summer monsoon (Asharaf et al. 2012; Ullah et al. 2020), and East Asian monsoon systems (Bao et al. 2010; Zuo and Zhang 2016).

However, the role of soil moisture in the TP thermal processes is not well understood up to date, and its possible link with SA monsoon remains unclear. In this study, using satellite-based derived soil moisture

and reanalysis data, we attempt to understand how the TP spring soil moisture influences the atmospheric thermal regimes and how these soil moisture-related regimes influence the SAH and the SA monsoon onset.

2 Study Area

The dominant topography of SA are the northern mountains that stretch from east to the northwest with an altitude of > 4000 meters (Fig. 1), and the topography in the central and southern regions are quite complex. The SA climate is diverse; the precipitation varies from 100 mm in the western region to > 1000 mm in the eastern region (Jain et al. 2013; Prabhu et al. 2017; Ullah et al. 2018a; Preethi et al. 2019). The monsoon precipitation mainly drives the hydrologic processes of the SA in summer and the western disturbances in winter. The air temperature shows quite similar spatial patterns as precipitation, with an average of 15℃ in the central region and more than 35℃ in the coastal region (Sheikh et al. 2015; Ullah et al. 2019a). SA is confronted with extreme weather events in the warming climate, which has threatened the livelihoods of more than 25% of the global population (Gu et al. 2012; Hou et al. 2014; Vemsani 2015).

TP serves as the source of perennial water supply into the main rivers of SA, and it can be termed as “water tank of SA” (Vemsani 2015). TP also influences the summer precipitation by inducing lower-level westerlies towards continental regions and preventing cold Siberian fronts in winter. The TP soil moisture follows a strong freeze/thaw cycle in winter and summer seasons (Ullah et al. 2018b); soil water thawing is initiated in April, and freezing is initiated in November (Su et al. 2011; Yang et al. 2013).

3 Data And Methods

3.1 Data

In-situ soil moisture observations over TP are limited, and thus satellite soil moisture from Special Sensor Microwave Imager (SSMI) is used in this study (Van Der Velde et al. 2014). This daily data, spanning 1988–2008 and expressed in volumetric water contents ($m^3\ m^{-3}$), is derived from SSM/I brightness temperature with a radiative transfer model (Semunegus et al. 2010; Van Der Velde et al. 2014). Comparisons with in-situ observations and reanalysis products have shown promising strength of the SSMI soil moisture in depicting the TP hydrological processes (Van Der Velde et al. 2014; Ullah et al. 2018b). The air temperature, geopotential height, and wind components are obtained from ERA-Interim, which is a global reanalysis product from ECMWF (European Centre for Medium-Range Weather Forecasts). ERA-Interim is upgraded from ERA-40 with a four-dimensional variation analysis scheme (4D-var), an improved atmospheric model, and an assimilation system (Dee et al. 2011). The spatial resolution of the ERA-Interim reanalysis is 0.75 degrees.

The precipitation data is obtained from Climate Hazards Group InfraRed Precipitation with Station (CHIRPS). CHIRPS is a combination of three different sources of precipitation products, including the IR-

derived precipitation merged with climatologies (CHPclim) and blended with station observations (Funk et al. 2015). The CHIRPS product has been validated in SA with a good performance during the monsoon season (Ullah et al. 2019b). The Modern-Era Retrospective analysis for Research and Application (MERRA-2) is used to estimate the TP's vertical diabatic heating profile. The temperature tendencies due to moist processes, radiation, and turbulent processes at multiple pressure levels were used to estimate the diabatic heating following (Chattopadhyay et al. 2013; Ullah et al. 2020). MERRA-2 is produced with Goddard Earth Observing System (GEOS-5) Atmospheric General Circulation Model version 5 by the National Aeronautics and Space Administration (NASA) Global Modelling and Assimilation Office (GMAO) (Rienecker et al. 2011). The strengths of MERRA-2 include its restructured assimilation system (Molod et al. 2012), an improved water balance, atmospheric physics, and glaciated land surface schemes (Robertson et al. 2014; Reichle et al. 2017).

The land surface heat fluxes were derived from the National Center for Environmental Prediction/Climate Forecast System Reanalysis (NCEP/CFSR) (Saha et al. 2010), including a coupled atmosphere-ocean-land model and an interactive sea-ice model. For the atmosphere, the Global Forecast System (GFS) model with a horizontal resolution of about 38km (T382) and 64 sigma pressure levels are used. The Noah land surface model and the coupled Geophysical Fluid Dynamics Laboratory Modular Ocean Model (GFDL MOM) version 4 are used for the land and ocean. For the current study, monthly mean fields of heat fluxes (sensible and latent heat), gridded at a resolution of 0.5°, are used (Kistler et al. 2001).

The Japanese 55-year Reanalysis (JRA-55) is used to study the vertical profile of latent and sensible heat fluxes of the TP (Wang et al. 2019a). Japanese 55-year Reanalysis is the second global reanalysis from the Japan Meteorological Agency (JMA) that spans from 1958 to present (Kobayashi et al. 2015). As an extension of JRA-25, the JRA-55 includes new historical quality-controlled observations, revised longwave radiation scheme, 4D-Var, and VarBC for satellite radiances. The JRA-55 is produced with the low-resolution (TL139) version of the JMA data assimilation system and aims to produce long-term reanalysis to better estimate multi-decadal climate variability. Recent studies have indicated the good performance of this data for the energy fluxes over the TP (Hu and Duan, 2015; Wang et al., 2019a)

3.2 Methods

South Asian monsoon onset is linked with an abrupt increase in precipitation magnitude, a seasonal reversal of winds, and a shift in heat maxima from the southern hemisphere to the northern hemisphere (Xavier et al. 2007; Wang et al. 2009; Puranik et al. 2013). Monsoon onset date is declared using these parameters individually or in combination (Zeng and Lu 2004; Wang et al. 2009; Stolbova et al. 2016). However, the localized nature of precipitation variability might be uncertain from region to region, resulting in a bogus monsoon onset date. The changes in wind shear and center of maximal heat reversal are relatively reliable for describing large-scale monsoon onset (Wang et al. 2001, 2009; Xavier et al. 2007). In this study, the monsoon onset indices representing wind shear and troposphere temperature gradient between the northern and southern hemispheres respectively and termed Wang Bin index (WB index hereon) and Xavier index (XV index hereon) (Wang et al. 2001, 2009; Xavier et al. 2007), are used.

The WB index is defined as the difference between 850hPa zonal wind averaged for (5°N 15°N, 40°E 80°E) and (20°N 30°N, 70°E 90°E), shown in Eq. (1). The monsoon onset date is declared when the wind shear between these two regions changes its sign from negative to positive for five consecutive days. The defined onset date represents changes in both circulation and precipitation, which exhibited a significant correlation with the subjective Indian monsoon onset index. The definition can be seen from Eq. (1),

$$\text{WB index} = \text{Average}\left(\left(U^{850hPa}_{5N-15N,\ 40E-80E}\right) - \left(U^{850hPa}_{20N-30N,\ 70E-90E}\right)\right) \quad (1)$$

The XV index is based on the tropospheric temperature gradient (averaged between 200hPa-600hPa) for the northern hemisphere (40–100°E, 5–35°N) and southern hemisphere (40–100°E, 15°S–5°N). The XV index is defined as the first day when the averaged tropospheric temperature (TT) gradient between the northern and southern hemisphere changes its sign from negative to positive. This index has less influence from the surface and boundary layer induced uncertainty and appeared to be significantly correlated with the Indian monsoon onset index. The definition can be seen from Eq. (2),

$$\text{XV index} = \text{Average}\left(\left(TT^{200hPa-600hPa}_{5N-35N,\ 40E-100E}\right) - \left(TT^{200hPa-600hPa}_{5N-15S,\ 40E-100E}\right)\right) \quad (2)$$

The SAH (South Asian High) is expressed as a persistent anticyclonic circulation system at 200hPa. The seasonal evolution influences the weather and climate of the Asian monsoon domain (Yongfu et al. 2002; Zhang et al. 2016; Ge et al. 2019). The SAH index (Eq. 3) is calculated from geopotential height at 200hPa averaged for (20°N 35°N, 40°E 115°E) during the spring season (April, May, and June) as specified by Zhang et al. (2016), and shown in Eq. (3),

$$\text{SAH index} = \text{Average}\left(Z^{200hPa}_{20N-35N,\ 40E-115E}\right) \quad (3)$$

In Eq. 3, Z indicates geopotential height at 200hPa for the respective region shown with latitude and longitude range, sensitive to TP's thermal heating and diabatic heating (Zhang et al. 2004; Rizou et al. 2015; Wu et al. 2015).

4 Results

4.1 Precipitation climatology

Figure 2 shows the climatology of monthly mean precipitation (Fig. 2a) and spatial precipitation pattern for the monsoon season (JJAS) (Fig. 2b) during 1988–2008. Figure 2 suggests that maximum precipitation is observed from June to September with a peak of > 200 mm in July. SA monsoon onset is partly in June; however, the whole SA experiences the monsoon onset in July, which continues till September. The spatial pattern of total precipitation in JJAS shows more precipitation in the north-eastern SA (Fig. 2b) with an amount of > 500 mm. It is reduced to about 300 mm in the central SA, and in western SA, it is less than 80mm. The monsoon onset across the region has been linked with several factors, including the sea surface temperature, westerlies progression, convection, and local continental-scale tipping elements. Less attention has been paid to the influence of the TP soil moisture-induced

thermal profile influence on the monsoon onset across time (Zhang et al. 2002; Stolbova et al. 2016; Ullah et al. 2020, 2021). The following section shows a diagnostic relationship of the soil moisture profile over the TP and its thermodynamics role in the SA monsoon onset.

4.2 Monsoon onset and soil moisture

The standardized SAH, the WB, and the XV indices are shown in Fig. 3. The positive WB and XV anomalies indicate late monsoon onset, and their negative anomalies indicate early monsoon onset, respectively. The XV index shows a negative correlation of -0.56 with the SAH index, the correlation between the WB index and the SAH is -0.61; both correlation coefficients have passed the significance test with a 95% confidence level. Thus, it is suggested that the SAH and the SA monsoon may have different mechanisms, and the SAH negatively affects the SA monsoon onset. These findings complement the previous studies and suggest that the SAH intensity may enhance the divergence aloft accompanied by lower-level cyclonic and convective activities, leading to monsoon onset vortex (MOV) in the SA monsoon domain (Liu et al. 2013; Wei et al. 2014). The TP thermal heating and energy fluxes are known to link with the SAH; however, the soil moisture relation with SAH remains unknown, although it is known to play an essential role in land surface energy fluxes partitioning.

Hence, a pixel-wise correlation analysis is conducted to understand the TP soil moisture relations with the WB, the XV, and the SAH index, respectively, and the results are shown in Fig. 4. The average soil moisture from April to June (AMJ) indicates springtime soil moisture over the TP (Ullah et al. 2020). It appears that both XV (Fig. 4a) and WB (Fig. 4b) indices are negatively correlated with springtime soil moisture across the TP, with correlation coefficients ranging from − 0.50 to -0.70. However, the SAH index is positively correlated with the springtime soil moisture across the plateau, and the correlation coefficients are ≥ 0.90 (α = 5%) in most areas. The TP soil moisture is hypothesized to modulate the SAH intensity through a certain mechanism, affecting the SA monsoon's onset. Several studies have indicated that soil moisture affects the boundary layer structure and the upper troposphere by altering the vertical thermal processes (Sanchez-Mejia and Papuga 2014; Koster et al. 2016; Berg et al. 2017; Schwingshackl et al. 2018). In the following sections, we have shown the spring soil moisture influence on the TP thermal profile and linked them with SAH movement and SA monsoon onset.

4.3 Spring soil moisture influence on TP thermal forcing

We conducted the composite analysis to understand the possible thermal processes that link the TP soil moisture to the SAH intensity and the SA monsoon onset. As shown in Fig. 3, the positive and negative values of the z-score indicate the deviation of the monsoon onset date from its climatological mean onset date. In this regard, the years with negative z-score values were referred to as early-onset composite (1990, 1999, 2002, and 2004) and late-onset composite (1992, 1995, 1997, and 2003) for positive z-score values, respectively. The respective average onset date/pentad for the early and late-onset years are further shown in Table 1. The onset timing estimated from the two indices has an obvious difference, implying that the onset inferred from zonal wind maybe earlier than tropospheric temperature. The onset composites have an evident difference of 20–25 days between the early and late-onset composite. The

monsoon onset's regionally indicating the reversal mechanism of the wind and tropospheric temperature, preceded by convective activities and abrupt precipitation in the Indian ocean, which moves towards continental regions in the following days (Liu et al. 2013). Based on these two composites, the TP's spring season thermodynamics is expressed as a precursor of the processes leading to the SAH modulation and the monsoon onset.

Table 1
Average monsoon onset days and the average monsoon onset pentad based on the composites.

Composite name	Years	XV index (onset day)	WB index (onset day)	Average onset pentad
	1990	134	128	26
	1999	140	130	27
Early onset	2002	135	127	26
	2004	136	126	26
	1992	162	157	32
Late onset	1995	152	159	31
	1997	156	163	32
	2003	152	163	32

The soil moisture, sensible heat, and latent heat anomalies in the spring season are analyzed in the early- and late-onset composites, respectively, shown in Fig. 5. In the early-onset composites, the TP soil moisture shows mostly positive anomalies (Fig. 5a) over the plateau; during the late-onset composites, the TP soil moisture shows negative anomalies across the plateau, except for the southeast corner (Fig. 5b). The associated thermal processes of the contrary composites are further studied. In the early-onset composite, the sensible heat fluxes (Fig. 5c) show negative anomalies of < -9 W m^2 in the eastern and southern TP, where the latent heat (Fig. 5e) shows strong positive anomalies with a magnitude of about 12 W m^{-2}. In the late-onset composite, the sensible heat (Fig. 5d) exhibited positive anomalies of 6 ~ 8 W m^{-2} in the eastern and the southern TP and negative anomalies from − 2 to -4 W m^{-2} in the northern TP. On the contrary, the latent heat (Fig. 5f) shows anomalies opposite to those of the TP's sensible heat.

Soil moisture plays an essential role in partitioning the available net radiation into sensible and latent heat, and the composite results agree with previous studies (Berg et al. 2015; Ford and Schoof 2016; Koster et al. 2016). Soil moisture deficit is suggested to increase the sensible heat and decrease the latent heat, although other factors such as solar forcing may affect these relations. However, the soil moisture influence on near-surface energy fluxes is rarely linked with the atmospheric profiles, local and remote-scale circulations using observational data. Hence, we further derived the vertical sensible and latent heat profiles in the early- and late-onset composites. Previous studies have indicated that the interannual variations of SAH are significantly affected by the condensation heating from the eastern TP and

Yangtze river valley (Wei et al. 2015; Zhang et al. 2016; Ge et al. 2019). Figure 6 shows the vertical profile of latent and sensible heat fluxes averaged for 27N to 37N and 85E to 103E. The vertical profile of latent and sensible heat fluxes is for the same region as used in the above studies, but consider the soil moisture effect rather than the precipitation-induced heating. In the early-onset composites (Fig. 6a), both sensible and latent heat anomalies are positive (0.8 K day^{-1}) near the surface; however, at mid-troposphere from 500 to 300 hPa, the sensible heat anomalies reduce to zero, and the latent heat anomalies are the strongest, reaching 2.5 K day^{-1}. In the late-onset composites (Fig. 6b), there are negative latent heat anomalies in the lower and upper troposphere from 400 to 200 hPa with a magnitude of <-0.7 K day^{-1}. The sensible heat flux during the late-onset composite is positive at near-surface (550 hPa) pressure levels (0.6 K day^{-1}). The sensible heat flux near the surface pressure level (600hPa) exhibited negative anomalies attributed to the surface and boundary layer induced gradients and uncertainties of the reanalysis products over TP (Cui and Wang 2009). During the frozen and transition period, the reanalysis products have shown deviations and uncertain states of the energy and water fluxes over the TP (Ullah et al. 2018) mainly due to deficiencies in model structures (Bi et al. 2016).

From Fig. 6, significant changes in latent and sensible heat fluxes in the early- and late-onset years are obvious from surface pressure levels till 200hPa. Considering the soil moisture role in modifying the energy fluxes in the overlying atmosphere through the convective processes (Taylor et al. 2011), a drier soil moisture profile may influence diabatic heating in the overlying atmosphere through enhancing the sensible heat flux and vice versa for the latent heat. On the other hand, the wetter soil enhances latent heat, releasing the absorbed excess energy upon condensation through an adiabatic ascent aloft (Koster et al. 2016). Over the TP, both sensible and latent heat fluxes are critically linked with the soil moisture's freeze-thaw stage during the transitional spring season (Cui and Wang 2009). They hence can actively influence the vertical profile of the diabatic heating over the plateau and produce divergent motion with lower/upper level cyclonic/anticyclonic pattern (Ullah et al. 2020).

The influence of soil moisture anomalies and, consequently, heat fluxes are also associated with the TP diabatic heating's vertical column. Figure 7 shows the vertical profiles of diabatic heating averaged from 27N to 38N in spring of the early-onset (Fig. 7a) and late-onset (Fig. 7b) composites. The diabatic heating has shown positive anomalies in the early-onset composites, which are more than > 1.2 K day^{-1} at central and eastern TP. On the contrary, in the late-onset composites, the diabatic heating shows negative anomalies of -0.4 K day^{-1} in the upper troposphere, whereas a consistent positive anomaly is evident in the eastern TP. The soil moisture anomalies affect the vertical profile of diabatic heating by partitioning the energy fluxes, which affects the overlying atmosphere where the excess energy absorbed is released (Koster et al. 2016). Such thermal influences are attributed to the land surface energy fluxes, which are sensitive to soil moisture anomalies (Cui and Wang 2009), and the enhanced latent heat anomalies result in a decreased boundary layer diabatic heating due to vertical adiabatic ascent. The diabatic heating anomalies in the eastern plateau favor unstable atmosphere and vertical ascent followed by descent in the western plateau. The mechanical forcing can be seen over the eastern plateau in the late-onset years

that potentially triggers a microscale wind ascent, and thus an increase in diabatic heating, as suggested by Wu et al. (2012) suggested.

Figure 8 shows the SAH anomalies at 200 hPa in the spring of the early-onset and the late-onset composites. In the early-onset composites (Fig. 8a), a high-pressure system prevails (> 18 gpm) over southwestern TP, which stretches towards Iranian Plateau (IP) and the Middle East. Another high-pressure system appears over the Eastern flank of TP, with the center over the Mongolian and Siberian regions. In the late-onset composites (Fig. 8b), the geopotential height in the SAH region shows obvious negative anomalies of <-16 gpm. Over the Indian Ocean and Northern Eurasian Continent, the strong high-pressure system is persistent with an increased geopotential height of > 10gpm. The high-pressure system apparent during the early monsoon onset composite is symmetrically replaced by a low-pressure system centered over the southern and northern TP with an intensity of <-18gpm each, respectively. The SAH (Fig. 8) has a consistently high and low-pressure mode in the spring of both early- and late-onset composites, varying in a tripole pattern. In the early-onset composite, the SAH exhibits two distinct high-pressure centers located at the TP's southern and northern sides, respectively. There is a low-pressure system over the Eurasian region, and hence a tripole pattern is formed. In the early-onset composite, the spring soil moisture-induced thermal forcing may intensify the SAH intensity. The wet soil moisture influences the vertical thermal column aloft through latent heat of condensation released, as Koster et al. (2016) described. In the late-onset composite's spring season, the vertical heating and energy fluxes over TP are weaker, which could be associated with surface energy and negative soil moisture anomalies. In response to the reduced thermal heating, the high-pressure centers at southern and northern TP are replaced by the low-pressure systems, whereas a high-pressure system replaces the Eurasian low-pressure system. The tripole pattern mechanism in monsoon onset is further explored with composites of vertical velocity and meridional wind components over TP.

Figure 9 shows the vertical velocity and meridional wind in the spring of the early- (**Fig .9a**) and late-onset (**Fig .9b**) composite. In the early-onset composite, an obvious ascending motion exists over the eastern plateau, which produces lower tropospheric cyclonic motion and diverges towards the western plateau. In the late-onset composite, an ascending motion is obvious at the western plateau, followed by a sinking motion at the eastern plateau. Figure 9 infers that in the spring season of the early monsoon onset composites, the intensified SAH favors wind ascent towards TP as evident in the eastern TP during early monsoon onset composites and vice versa for the delayed onset composites. The ascent/descent is vastly linked with the convergence of winds from the Indian ocean, including a land-atmosphere ocean thermal contrast, leading to monsoon onset and precipitation (Wu et al. 2012; Pathak et al. 2017a). In the following section, a pentad-scale movement of the SAH and its associated ascent over the TP is linked with the transition of the equatorial zonal easterlies into prevailing westerlies resulting in monsoon onset due to strong convective activities and precipitation in the SA monsoon domain.

4.4 SAH zonal movement and monsoon onset

Figure 10 shows the pentad evolution of the SAH for early and late monsoon onset composites during the SA monsoon onset phase. For both early and late-onset composites, two pentads, including the pre-onset

(onset pentad: -1) and onset-pentad (onset pentad: 0), were selected as an indicator of the SAH location and short-term evolution. During the early onset composite, in the pre-onset pentad (Fig. 10a), the SAH center is located over TP stretched zonally with a weak low located westward of the plateau. Such a high(low) combination indicates a strong ascending motion over TP accompanied by an intensified sinking west of the plateau. From the onset pentad (Fig. 10b), the SAH centers of the SAH move northeastward with secondary high generated over Iranian Plateau. The northeastward movement indicates the downstream convective activities initiation in the Bay of Bengal (BOB) due to monsoon onset and establishment of the westerlies and easterlies into the region (Liu et al. 2013). During the late-onset composite, in the post-onset (Fig. 10c) the SAH low is centered over the Iranian plateau extending into the SA in the east, indicating a stable high pressure in the lower troposphere. The TP high-pressure system is farther northwest of the plateau, indicating a weaker ascent. During the onset pentad (Fig. 10d), the two low-pressure systems located eastward of the plateau and over the Iranian plateau replace the SAH centers, as evident during the early onset pentad. The northwest high center of the SAH moves into TP, but weaker intensity indicates an ascent over continental regions located westward of the Bay of Bengal. In conclusion, two aspects of the SAH are evident during the early and late-onset composites. The first aspect is its potential relationship with TP soil moisture induced thermal forcing that maintains its intensity and controls the monsoon onset. The second aspect of the SAH is its expansion into the high latitudes, which intensify the meridional circulations. Hence, it can be the potential reason for early monsoon onset triggered by TP soil moisture-induced thermal forcing. The findings complement the previous studies reporting similar characteristics of the SAH (Wu 2002; Wei et al. 2014); however, a model study will further be conducted to validate the findings.

Figure 11 shows the TP meridional wind component, and vertical velocity averaged for the latitudinal range of 27N to 38N across the longitude. During the pre-onset pentad (Fig. 11a), the western and central plateau experience an intensified ascent accompanied by descent in the western plateau, which during the onset-pentad (Fig. 11b) moves eastward into the eastern plateau and Bay of Bengal region. In the onset-pentad, the ascending motion over the eastern plateau results in the regional westerlies and easterlies movement towards the SA domain that initiates in the Bay of Bengal and pushes the SAH to the north. A similar pattern of the ascending motion and upper-tropospheric divergent motion was also reported by Ullah et al. (2020) and Liu et al. (2013), attributed to the plateau soil moisture thermal profile and condensation heating release. During late-onset composite, the pre-onset pentad (Fig. 11c) meridional wind and vertical velocity anomalies are weaker with obvious descending motion evident over the plateau, inferring a weaker thermal profile of the plateau. The onset pentad (Fig. 11d) has experienced a relatively weaker ascent over the western plateau and Yangtze river basin but rather a stronger descent over the eastern plateau. Such weaker ascent and partly descent over the eastern plateau can potentially be attributed to soil moisture negative anomalies that can lead to weaker thermal profile and westward shift in the ascent and associated precipitation. To explore the regional westerlies and easterlies convergence into the SA monsoon domain forced by TP soil moisture-laden thermal forcing, the lower tropospheric wind anomalies and vertical velocity are shown at 850 hPa. The wind anomalies shown are

a representation of the monsoon onset due to wind shear in the pre-defined monsoon index (WB-index) representing the westerlies evolution replacing the zonal easterlies.

Figure 12 shows the wind components (vectors) and vertical velocity (shaded) for the pre-onset, onset, and post-onset pentads for the early and late-onset composites at 850 hPa. The wind anomalies are used to show the transition of the westerlies and establishment of the subtropical jet stream associated with enhanced moisture contents, enhanced convective activities, and ascent showed by vertical velocity anomalies. During early-onset composites, in the pre-onset pentad (Fig. 12a), the prominent features include zonal easterlies from the pacific warm pool and north-easterlies from South China Sea (SCS) enters into Indian ocean and Bay of Bengal (BOB). These two easterlies merge into the continental westerlies and form prevailing continental easterlies gusting towards eastern Africa. In the onset pentad (Fig. 12c), the equatorial zonal easterlies after entering into Indian ocean changes into zonal westerlies, and the SCS currents after entering into BOB, join the zonal westerlies and advances into the continental landmasses. In the onset pentad, a clear transition of the easterlies into westerlies is evident with stronger intensities and ascent (shaded) in the Indian ocean and peninsular India, which is relatively weaker in the continental regions. During the post-onset pentad (Fig. 12e), the south-westerlies from the Indian ocean and zonal easterlies intensify the ascent, evident from vertical velocity in the continental regions. During the pre-onset pentad of late-onset (Fig. 12b), the zonal equatorial easterlies are much weaker, and south-westerlies also replace the SCS north-easterlies with stable atmosphere and descending motion evident in BOB and Arabian sea. In the onset-pentad (Fig. 12d), the zonal easterlies change into westerlies and advance towards SA, but the BOB easterlies are suppressed, and hence a south-westerlies jet into SCS prevails. In the post-onset pentad (Fig. 12f), the westerlies are fully established but rather weaker and limited to the western parts of SA with stable conditions over BOB. In conclusion, the TP soil moisture can influence the ascent and SAH intensity and modulation in zonal and meridional domains that exhibit teleconnections with downstream zonal and meridional wind and modulate the monsoon onset. The findings agree with previous studies suggesting that TP thermal profile has a strong influence on the Asian monsoon by changing the circulation patterns and thus precipitation magnitude (Wu et al. 2012; Rajagopalan and Molnar 2013; Ullah et al. 2020). From the composite analysis, it can be deduced that spring soil moisture anomalies over TP influence the near-surface energy balance, which can further affect TP energy fluxes, the vertical profile of diabatic heating aloft (Wu et al. 2012; Wang et al. 2014). Such thermal conditions can affect the SAH intensity, which results in the high/low-pressure centers across southern/northern TP. The SAH variability can trigger vertical ascending/descending motion, leading to cyclonic/anticyclonic activities, and thus modulate the SA monsoon onset.

5 Summary And Discussion

The Tibetan Plateau thermodynamics are studied and linked with regional and large-scale climate phenomena using empirical and numerical models (Wu et al. 2012; He et al. 2019). Soil moisture role is least explored in the thermal effects of TP due to limited observations. The current study has used remotely sensed soil moisture during 1988–2008 to study soil moisture role in the Monsoon onset over South Asia (SA). The Monsoon onset over SA is usually associated with an abrupt change in

precipitation, wind shear, and tropospheric heat maxima, on which the monsoon onset indices are generally based. In this study, the monsoon onset indices, which represent large-scale monsoon onset dynamics, are used (Wang et al. 2001; Xavier et al. 2007). The South Asian High (SAH) index is considered for its sensitivity to TP thermal heating and can affect the onset of Asian monsoon (Liu et al. 2013; Zhang et al. 2016; Ge et al. 2019).

A significant positive correlation was observed from the results for spring soil moisture (April, May, and June) and SAH index; furthermore, both SAH and soil moisture exhibited a significant negative correlation with WB and XV monsoon onset indices. The underlying mechanism between the monsoon onset and SAH and TP soil moisture is explored for early-onset (1990, 1999, 2002, and 2004) and late-onset (1992, 1995, 1997, and 2003) composites, respectively. In the early-onset composite, the spring soil moisture has shown obvious positive anomalies in the eastern TP and vice versa in late-onset years. In response to soil moisture anomalies, a consistent positive/negative latent/sensible heat anomaly is persistent in the early-/late-onset composite, which infers that soil moisture has a substantial energy flux role partitioning. The findings are consistent with previous studies that near-surface energy partitioning is sensitive to soil moisture dynamics (Li and Ma 2015; Koster et al. 2016; Wang et al. 2017b). The vertical profile of heat fluxes showed consistent dynamics with positive latent heat anomalies and negative sensible heat anomalies in the early-onset years. In contrast, latent heat is rather negative with dry soil moisture conditions in the late-onset years, and sensible heat flux is enhanced in the lower pressure level and reduced in the upper troposphere. In a series of studies on a global scale, soil moisture is reported to influence the boundary layer processes, diabatic heating anomalies, divergent motion locally and in results, influence the local and remote climate fields through changing the stream function, precipitation, and near-surface climate fields (Koster et al. 2016; Ullah et al. 2020). The feedback and interaction loop involves soil moisture translates into surface energy and temperature anomalies extending to the upper troposphere through a chain of coupling and induce high and low-pressure systems (Seneviratne et al. 2010).

The amount of solar radiation over TP is relatively higher due to its altitude and lower air pressure, so the climate dynamics over the region are different than the surroundings (Anmin et al. 2012; Zhou et al. 2018). A seasonal freeze-thaw cycle of the plateau has a significant role in affecting the energy fluxes, which are linked with soil moisture magnitude (Cui and Wang 2009). Previous studies have indicated the essential role of soil moisture in partitioning the available solar energy into sensible and latent heat (Koster et al. 2016; Berg et al. 2017; Schwingshackl et al. 2018), and consequently affecting the boundary layer height (Sanchez-Mejia and Papuga 2014). From the diabatic and adiabatic processes, the energy is transferred to the upper troposphere, producing a center of high and low pressure, which is obvious in TP’s composite analysis. The diabatic heating profile in the early-onset composite is higher; this could be associated with the surface latent heat fluxes, which are released during the ascending motion enhancing the diabatic heating and influencing the circulations and divergent motion (Koster et al. 2016; Ullah et al. 2020). In the late-onset years, the diabatic heating is rather weaker and possibly implies that dry surface conditions may favor dry adiabatic processes and hence a decrease in the upper tropospheric heating. The proposed mechanism may be attributed to multiple processes and may not only depend on soil

moisture; however, further studies with model experiments will better delineate the underlying mechanism. In a previous study, similar local feedback between soil moisture precipitation is reported with a strong correlation between eastern plateau spring soil moisture and TP monsoon precipitation involving a similar mechanism observed in the current study (Zhou et al. 2018).

The latent heat of condensation over eastern TP enhances the diabatic heating and leads to strong vertical ascending motion (Anmin et al. 2012; Zhang et al. 2016; Zhou et al. 2018). In spring, TP's energy profile can be largely attributed to soil moisture anomalies; thus, the energy released may also be subjected to soil moisture, which resulted from winter snow cover and springtime precipitation. The diabatic heating can enhance or suppress the magnitude of vertical ascending motion, leading to lower atmospheric cyclonic and anticyclonic circulations and vice versa (Wang et al. 2014, 2019a). With ascending and descending wind motions, the TP tropospheric pressure pattern varies (Zhang et al. 2016; Ge et al. 2019), affecting the SAH intensity in a distinct tripole pattern. These large-scale tropospheric variabilities affect the mid-tropospheric wind shear and tropospheric thermal profiles. The SA monsoon onset is associated with changes in wind shears and heat maxima from the southern hemisphere towards the northern hemisphere. During the early onset pentad, the SAH move towards the east, and during the onset pentad moves towards the northeast; such zonal and meridional movement of the SAH are previously reported as an indication of the monsoon onset initiation in BOB proceeded by a continental increase in precipitation (Liu et al. 2013). The plateau's divergent motion (Ullah et al. 2020) appeared to link the soil moisture as thermal heat source that triggers above normal diabatic heating existence, leading to intensified ascent and early onset, which is weaker in the later onset composite. The 850 hPa wind components transition from prevailing easterlies during the pre-onset pentad to westerlies in the onset-pentad accompanied by enhanced convection and ascent is showing the teleconnections of the plateau soil moisture-induced thermal profile with regional circulations in the SCS, western Pacific, and Indian ocean.

In conclusion, this study has shown an empirical linkage between TP soil moisture anomalies and SA monsoon onset through thermal processes. The thermal processes associated with soil moisture anomalies affect the SAH variability and, consequently, the SA monsoon onset. The monsoon onset and physical processes are subjected to annual and decadal variability, including external forcing and internal forcing such as oceanic forcing, including the ENSO and IOD influence (Wang et al. 2017a). The intraseasonal oscillations of air-land-sea interactions and their coupling with Asian monsoon are still unclear and require further studies (Liu et al. 2013). However, such observed linkages are empirical, and further numerical experiments are expected to improve our understanding of TP soil moisture's role in modulating the SA monsoon onset.

Declarations

Acknowledgments

This study is financially supported by the National Key Research and Development Program of China (2017YFA0603701), the National Natural Science Foundation of China (41875094), the Sino-German Cooperation Group Program (GZ1447), and the China Scholarship Council.

Conflict of Interest:

The authors declare that they have no conflict of interest.

References

1. Abe M, Hori M, Yasunari T, Kitoh A (2013) Effects of the Tibetan Plateau on the onsetof the summer monsoon in South Asia: The role of the air-sea interaction. J Geophys Res Atmos 118:1760–1776. doi: 10.1002/jgrd.50210
2. Anmin D, Wu G, Liu Y, et al (2012) Weather and Climate Effects of the Tibetan Plateau. Adv Atmos Sci 29:978–992. doi: 10.1007/s00376-012-1220-y.1.Introduction
3. Asharaf S, Dobler A, Ahrens B (2012) Soil Moisture–Precipitation Feedback Processes in the Indian Summer Monsoon Season. J Hydrometeorol. doi: 10.1175/JHM-D-12-06.1
4. Bao Q, Liu Y, Shi J, Wu G (2010) Comparisons of soil moisture datasets over the Tibetan Plateau and application to the simulation of Asia summer monsoon onset. Adv Atmos Sci 27:303–314. doi: 10.1007/s00376-009-8132-5
5. Berg A, Lintner B, Findell K, Giannini A (2017) Soil moisture influence on seasonality and large-scale circulation in simulations of the West African monsoon. J Clim 30:2295–2317. doi: 10.1175/JCLI-D-15-0877.1
6. Berg A, Lintner BR, Findell K, et al (2015) Interannual coupling between summertime surface temperature and precipitation over land: Processes and implications for climate change. J Clim 28:1308–1328. doi: 10.1175/JCLI-D-14-00324.1
7. Bi H, Ma J, Zheng W, Zeng J (2016) Comparison of soil moisture in GLDAS model simulations and in situ observations over the Tibetan Plateau. J Geophys Res Atmos 121:2658–2678. doi: 10.1002/2015JD024131
8. Chattopadhyay R, Sur S, Joseph S, Sahai AK (2013) Diabatic heating profiles over the continental convergence zone during the monsoon active spells. Clim Dyn 41:205–226. doi: 10.1007/s00382-013-1739-3
9. Cui Y, Wang C (2009) Comparison of sensible and latent heat fluxes during the transition season over the western Tibetan Plateau from reanalysis datasets. Prog Nat Sci 19:719–726. doi: 10.1016/j.pnsc.2008.11.001
10. Dee DP, Uppala SM, Simmons AJ, et al (2011) The ERA-Interim reanalysis: configuration and performance of the data assimilation system. Q J R Meteorol Soc 137:553–597. doi: 10.1002/qj.828
11. Duan A, Sun R, He J (2017) Impact of surface sensible heating over the Tibetan Plateau on the western Pacific subtropical high: A land–air–sea interaction perspective. Adv Atmos Sci 34:157–

168. doi: 10.1007/s00376-016-6008-z

12. Ford TW, Schoof JT (2016) Oppressive Heat Events in Illinois Related to Antecedent Wet Soils. J Hydrometeorol 17:2713–2726. doi: 10.1175/jhm-d-16-0075.1
13. Funk C, Peterson P, Landsfeld M, et al (2015) The climate hazards infrared precipitation with stations - A new environmental record for monitoring extremes. Sci Data 2:1–21. doi: 10.1038/sdata.2015.66
14. Ge J, You Q, Zhang Y (2019) Effect of Tibetan Plateau heating on summer extreme precipitation in eastern China. Atmos Res 218:364–371. doi: S0169809518309062
15. Ge J, You Q, Zhang Y (2018) Interannual variation of the northward movement of the South Asian High towards the Tibetan Plateau and its relation to the Asian Summer Monsoon onset. Atmos Res 213:381–388. doi: 10.1016/j.atmosres.2018.06.026
16. Gu H, Wang G, Yu Z, Mei R (2012) Assessing future climate changes and extreme indicators in east and south Asia using the RegCM4 regional climate model. Clim Change 114:301–317. doi: 10.1007/s10584-012-0411-y
17. He B, Liu Y, Wu G, et al (2019) The role of air–sea interactions in regulating the thermal effect of the Tibetan–Iranian Plateau on the Asian summer monsoon. Clim Dyn 52:4227–4245. doi: 10.1007/s00382-018-4377-y
18. Hou AY, Kakar RK, Neeck S, et al (2014) The Global Precipitation Measurement (GPM) Mission. Bull Am Meteorol Soc. doi: 10.1175/BAMS-D-13-00164.1
19. Hu J, Duan A (2015) Relative contributions of the Tibetan Plateau thermal forcing and the Indian Ocean Sea surface temperature basin mode to the interannual variability of the East Asian summer monsoon. Clim Dyn 45:2697–2711. doi: 10.1007/s00382-015-2503-7
20. Huang JJ, Zhang N, Choi G, et al (2018) Spatiotemporal Patterns and Trends of Precipitation and Their Correlations with Related Meteorological Factors by Two Sets of Reanalysis Data in China. Hydrol Earth Syst Sci Discuss 5:1–35. doi: 10.5194/hess-2017-756
21. Jain SK, Kumar V, Saharia M (2013) Analysis of rainfall and temperature trends in northeast India. Int J Climatol 33:968–978. doi: 10.1002/joc.3483
22. Kistler R, Kalnay E, Collins W, et al (2001) The NCEP-NCAR 50-year reanalysis: Monthly means CD-ROM and documentation. Bull Am Meteorol Soc 82:247–267. doi: 10.1175/1520-0477(2001)082<0247:TNNYRM>2.3.CO;2
23. Kobayashi S, Ota Y, Harada Y, et al (2015) The JRA-55 Reanalysis: General Specifications and Basic Characteristics. J Meteorol Soc Japan Ser II 93:5–48. doi: 10.2151/jmsj.2015-001
24. Koster RD, Chang Y, Wang H, Schubert SD (2016) Impacts of local soil moisture anomalies on the atmospheric circulation and on remote surface meteorological fields during boreal summer: A comprehensive analysis over North America. J Clim 29:7345–7364. doi: 10.1175/JCLI-D-16-0192.1
25. Li M, Ma Z (2015) Sensible and Latent Heat Flux Variability and Response to Dry–Wet Soil Moisture Zones Across China. Boundary-Layer Meteorol 154:157–170. doi: 10.1007/s10546-014-9963-x

26. Liu B, Wu G, Mao J, He J (2013) Genesis of the South Asian high and its impact on the Asian summer monsoon onset. J Clim 26:2976–2991. doi: 10.1175/JCLI-D-12-00286.1
27. Liu Y, Wu G, Hong J, et al (2012) Revisiting Asian monsoon formation and change associated with Tibetan Plateau forcing: II. Change. Clim Dyn 39:1183–1195. doi: 10.1007/s00382-012-1335-y
28. Lu M, Yang S, Li Z, et al (2017) Possible effect of the Tibetan Plateau on the “upstream” climate over West Asia, North Africa, South Europe and the North Atlantic. Clim Dyn 0:1–14. doi: 10.1007/s00382-017-3966-5
29. Molod A, Takacs L, Suarez M, et al (2012) The GEOS-5 Atmospheric General Circulation Model: Mean Climate and Development from MERRA to Fortuna
30. Naidu C V., Dharma Raju A, Vinay Kumar P, Satyanarayana GC (2017) Perceptible changes in Indian summer monsoon rainfall in relation to Indian Monsoon Index. Glob Planet Change 157:83–92. doi: 10.1016/j.gloplacha.2017.08.016
31. Park H-S, Chiang JCH, Bordoni S (2012) The Mechanical Impact of the Tibetan Plateau on the Seasonal Evolution of the South Asian Monsoon. J Clim 25:2394–2407. doi: 10.1175/JCLI-D-11-00281.1
32. Pathak A, Ghosh S, Alejandro Martinez J, et al (2017a) Role of oceanic and land moisture sources and transport in the seasonal and interannual variability of summer monsoon in India. J Clim 30:1839–1859. doi: 10.1175/JCLI-D-16-0156.1
33. Pathak A, Ghosh S, Kumar P, Murtugudde R (2017b) Role of Oceanic and Terrestrial Atmospheric Moisture Sources in Intraseasonal Variability of Indian Summer Monsoon Rainfall. Sci Rep 7:1–11. doi: 10.1038/s41598-017-13115-7
34. Prabhu A, Oh J, Kim I, et al (2017) Summer monsoon rainfall variability over North East regions of India and its association with Eurasian snow, Atlantic Sea Surface temperature and Arctic Oscillation. Clim Dyn 49:2545–2556. doi: 10.1007/s00382-016-3445-4
35. Preethi B, Ramya R, Patwardhan SK, et al (2019) Variability of Indian summer monsoon droughts in CMIP5 climate models. Clim Dyn. doi: 10.1007/s00382-019-04752-x
36. Puranik SS, Sinha Ray KC, Sen PN, Pradeep Kumar P (2013) An index for predicting the onset of monsoon over Kerala. Curr Sci 105:954–961
37. Rajagopalan B, Molnar P (2013) Signatures of Tibetan Plateau heating on Indian summer monsoon rainfall variability. J Geophys Res Atmos 118:1170–1178. doi: 10.1002/jgrd.50124
38. Reichle RH, Draper CS, Liu Q, et al (2017) Assessment of MERRA-2 land surface hydrology estimates. J Clim 30:2937–2960. doi: 10.1175/JCLI-D-16-0720.1
39. Rienecker MM, Suarez MJ, Gelaro R, et al (2011) MERRA: NASA’s modern-era retrospective analysis for research and applications. J Clim 24:3624–3648. doi: 10.1175/JCLI-D-11-00015.1
40. Rizou D, Flocas HA, Athanasiadis P, Bartzokas A (2015) Relationship between the Indian summer monsoon and the large-scale circulation variability over the Mediterranean. Atmos Res 152:159–169. doi: 10.1016/j.atmosres.2014.07.021

41. Robertson FR, Bosilovich MG, Roberts JB, et al (2014) Consistency of Estimated Global Water Cycle Variations over the Satellite Era. J Clim 27:6135–6154. doi: 10.1175/JCLI-D-13-00384.1
42. Saha S, Moorthi S, Pan H-L, et al (2010) The NCEP Climate Forecast System Reanalysis. Bull Am Meteorol Soc 91:1015–1058. doi: 10.1175/2010bams3001.1
43. Sanchez-Mejia ZM, Papuga SA (2014) Observations of a two-layer soil moisture influence on surface energy dynamics and planetary boundary layer characteristics in a semiarid shrubland. Water Resour Res 50:306–317. doi: 10.1002/2013WR014135
44. Schwingshackl C, Hirschi M, Seneviratne SI (2018) A theoretical approach to assess soil moisture–climate coupling across CMIP5 and GLACE-CMIP5 experiments. Earth Syst Dyn Discuss 1–26. doi: 10.5194/esd-2018-34
45. Semunegus H, Berg W, Bates JJ, et al (2010) An Extended and Improved Special Sensor Microwave Imager (SSM/I) Period of Record. J Appl Meteorol Climatol 49:424–436. doi: 10.1175/2009JAMC2314.1
46. Seneviratne SI, Corti T, Davin EL, et al (2010) Investigating soil moisture-climate interactions in a changing climate: A review. Earth-Science Rev 99:125–161. doi: 10.1016/j.earscirev.2010.02.004
47. Sheikh MM, Manzoor N, Ashraf J, et al (2015) Trends in extreme daily rainfall and temperature indices over South Asia. Int J Climatol 35:1625–1637. doi: 10.1002/joc.4081
48. Stolbova V, Surovyatkina E, Bookhagen B, Kurths J (2016) Tipping elements of the Indian monsoon: Prediction of onset and withdrawal. Geophys Res Lett 43:3982–3990. doi: 10.1002/2016GL068392
49. Su Z, Wen J, Dente L, et al (2011) The tibetan plateau observatory of plateau scale soil moisture and soil temperature (Tibet-Obs) for quantifying uncertainties in coarse resolution satellite and model products. Hydrol Earth Syst Sci 15:2303–2316. doi: 10.5194/hess-15-2303-2011
50. Taylor CM, Parker DJ, Kalthoff N, et al (2011) New perspectives on land-atmosphere feedbacks from the African Monsoon Multidisciplinary Analysis. Atmos Sci Lett 12:38–44. doi: 10.1002/asl.336
51. Ullah S, You Q, Ali A, et al (2019a) Observed changes in maximum and minimum temperatures over China- Pakistan economic corridor during 1980–2016. Atmos Res 216:37–51. doi: 10.1016/j.atmosres.2018.09.020
52. Ullah S, You Q, Ullah W, Ali A (2018a) Observed changes in precipitation in China-Pakistan economic corridor during 1980–2016. Atmos Res 210:1–14. doi: 10.1016/j.atmosres.2018.04.007
53. Ullah W, Guojie W, Gao Z, et al (2020) Observed linkage between Tibetan Plateau soil moisture and South Asian summer precipitation and the possible mechanism. J Clim 34:1–1. doi: 10.1175/jcli-d-20-0347.1
54. Ullah W, Guojie W, Lou D, et al (2021) Large-scale atmospheric circulation patterns associated with extreme monsoon precipitation in Pakistan during 1981–2018. Atmos Res 253:105489. doi: 10.1016/j.atmosres.2021.105489
55. Ullah W, Wang G, Ali G, et al (2019b) Comparing Multiple Precipitation Products against In-Situ Observations over Different Climate Regions of Pakistan. Remote Sens 11:628. doi: 10.3390/rs11060628

56. Ullah W, Wang G, Gao Z, et al (2018b) Comparisons of remote sensing and reanalysis soil moisture products over the Tibetan Plateau, China. Cold Reg Sci Technol 146:110–121. doi: 10.1016/j.coldregions.2017.12.003
57. Van Der Velde R, Salama MS, Pellarin T, et al (2014) Long term soil moisture mapping over the Tibetan plateau using special sensor microwave/imager. Hydrol Earth Syst Sci 18:1323–1337. doi: 10.5194/hess-18-1323-2014
58. Vemsani L (2015) The Himalayan Ranges, Glaciers, Lakes and Rivers: An International Ecological, Economic and Military Outlook. In: Webb MJ, Wijeweera A (eds) The Political Economy of Conflict in South Asia. Palgrave Macmillan UK, London, pp 171–190
59. Wang B, Ding Q, Joseph P V. (2009) Objective definition of the Indian summer monsoon onset. J Clim 22:3303–3316. doi: 10.1175/2008JCLI2675.1
60. Wang B, Fan Z (1999) Choice of South Asian Summer Monsoon Indices. Bull Am Meteorol Soc 80:629–638. doi: 10.1175/1520-0477(1999)080<0629:COSASM>2.0.CO;2
61. Wang B, Wu R, Lau KM (2001) Interannual variability of the asian summer monsoon: Contrasts between the Indian and the Western North Pacific-East Asian monsoons. J Clim 14:4073–4090. doi: 10.1175/1520-0442(2001)014<4073:IVOTAS>2.0.CO;2
62. Wang PX, Wang B, Cheng H, et al (2017a) The global monsoon across time scales: Mechanisms and outstanding issues. Earth-Science Rev 174:84–121. doi: 10.1016/j.earscirev.2017.07.006
63. Wang Q, Zhang T, Jin H, et al (2017b) Observational study on the active layer freeze–thaw cycle in the upper reaches of the Heihe River of the north-eastern Qinghai-Tibet Plateau. Quat Int 440:13–22. doi: 10.1016/j.quaint.2016.08.027
64. Wang S, Mo X, Liu S, et al (2016a) Validation and trend analysis of ECV soil moisture data on cropland in North China Plain during 1981–2010. Int J Appl Earth Obs Geoinf 48:110–121. doi: 10.1016/j.jag.2015.10.010
65. Wang Z, Duan A, Wu G (2014) Time-lagged impact of spring sensible heat over the Tibetan Plateau on the summer rainfall anomaly in East China: Case studies using the WRF model. Clim Dyn 42:2885–2898. doi: 10.1007/s00382-013-1800-2
66. Wang Z, Duan A, Wu G, Yang S (2016b) Mechanism for occurrence of precipitation over the southern slope of the Tibetan Plateau without local surface heating. Int J Climatol 36:4164–4171. doi: 10.1002/joc.4609
67. Wang Z, Yang S, Duan A, et al (2019a) Tibetan Plateau heating as a driver of monsoon rainfall variability in Pakistan. Clim Dyn 52:6121–6130. doi: 10.1007/s00382-018-4507-6
68. Wang Z, Yang S, Duan A, et al (2019b) Tibetan Plateau heating as a driver of monsoon rainfall variability in Pakistan. Clim Dyn 52:6121–6130. doi: 10.1007/s00382-018-4507-6
69. Wei W, Zhang R, Wen M, et al (2015) Interannual variation of the South Asian high and its relation with Indian and east asian summer monsoon rainfall. J Clim 28:2623–2634. doi: 10.1175/JCLI-D-14-00454.1

70. Wei W, Zhang R, Wen M, et al (2014) Impact of Indian summer monsoon on the South Asian High and its influence on summer rainfall over China. Clim Dyn 43:1257–1269. doi: 10.1007/s00382-013-1938-y
71. Wu G, He B, Liu Y, et al (2015) Location and variation of the summertime upper-troposphere temperature maximum over South Asia. Clim Dyn 45:2757–2774. doi: 10.1007/s00382-015-2506-4
72. Wu G, Liu Y, He B, et al (2012) Thermal Controls on the Asian Summer Monsoon. Sci Rep 2:404. doi: 10.1038/srep00404
73. Wu G, Liu Y, Zhang Q, et al (2007) The Influence of Mechanical and Thermal Forcing by the Tibetan Plateau on Asian Climate. J Hydrometeorol 8:770–789. doi: 10.1175/jhm609.1
74. Wu G, Zhang Y (1998) Tibetan Plateau forcing and the timing of the monsoon onset over South Asia and the South China Sea. Mon Weather Rev 126:913–927. doi: 10.1175/1520-0493(1998)126<0913:TPFATT>2.0.CO;2
75. Wu R (2002) A mid-latitude Asian circulation anomaly pattern in boreal summer and its connection with the Indian and East Asian summer monsoons. Int J Climatol. doi: 10.1002/joc.845
76. Xavier PK, Marzin C, Goswami BN (2007) An objective definition of the Indian summer monsoon season and a new perspective on the ENSO–monsoon relationship. Q J R Meteorol Soc 133:749–764. doi: 10.1002/qj.45
77. Xie X, Duan A, Shi Z, et al (2020) Modulation of surface sensible heating over the Tibetan Plateau on the interannual variability of East Asian dust cycle. 1–29
78. Yang K, Qin J, Zhao L, et al (2013) A multiscale soil moisture and freeze-thaw monitoring network on the third pole
79. Yongfu Q, Qiong Z, Yonghong Y, Xuchong Z (2002) Seasonal Variation and Heat Preference of the South Asia High. Adv Atmos Sci 19:821–836. doi: 10.1007/s00376-002-0047-3
80. Zeng X, Lu E (2004) Globally Unified Monsoon Onset and Retreat Indexes. J Clim 17:2241–2248. doi: 10.1175/1520-0442(2004)017<2241:gumoar>2.0.co;2
81. Zhang P, Liu Y, He B (2016) Impact of East Asian summer monsoon heating on the interannual variation of the South Asian high. J Clim 29:159–173. doi: 10.1175/JCLI-D-15-0118.1
82. Zhang Q, WU G, Qian Y (2004) The Bimodality of the 100 hPa South Asia High and its Relationship to the Climate Anomaly over East Asia in Summer. J Meteorol Soc Japan 80:733–744. doi: 10.2151/jmsj.80.733
83. Zhang Y, Li T, Wang B, Wu G (2002) Onset of the summer monsoon over the Indochina Peninsula: Climatology and interannual variations. J Clim. doi: 10.1175/1520-0442(2002)015<3206:OOTSMO>2.0.CO;2
84. Zhou J, Wen J, Liu R, et al (2018) Late spring soil moisture variation over the Tibetan Plateau and its influences on the plateau summer monsoon. Int J Climatol 1–13. doi: 10.1002/joc.5723
85. Zuo Z, Zhang R (2016) Influence of soil moisture in eastern China on the East Asian summer monsoon. Adv Atmos Sci 33:151–163. doi: 10.1007/s00376-015-5024-8

Figures

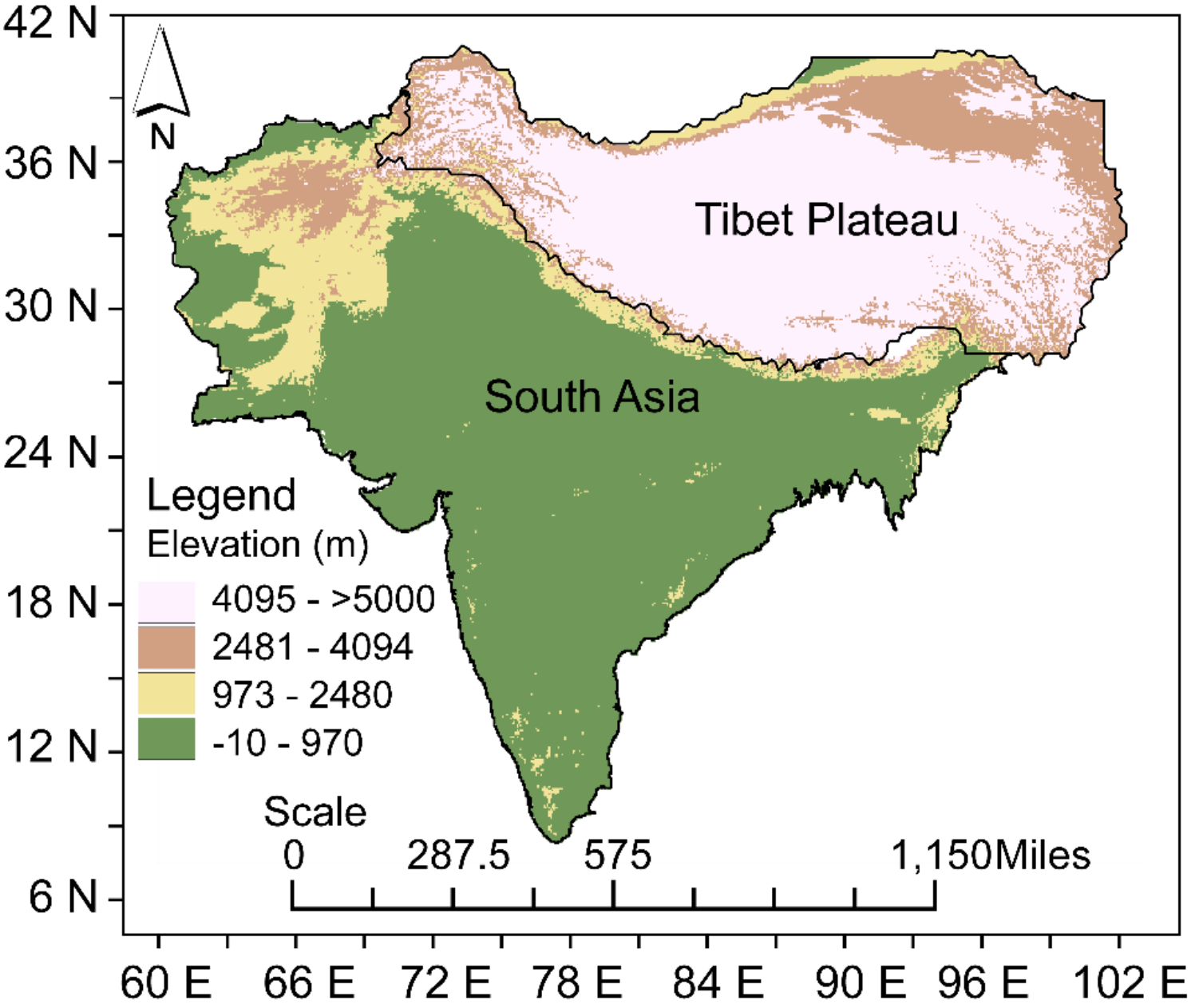

Figure 1

Topographic map of South Asia and Tibet Plateau showing its altitude classes. Note: The designations employed and the presentation of the material on this map do not imply the expression of any opinion whatsoever on the part of Research Square concerning the legal status of any country, territory, city or area or of its authorities, or concerning the delimitation of its frontiers or boundaries. This map has been provided by the authors.

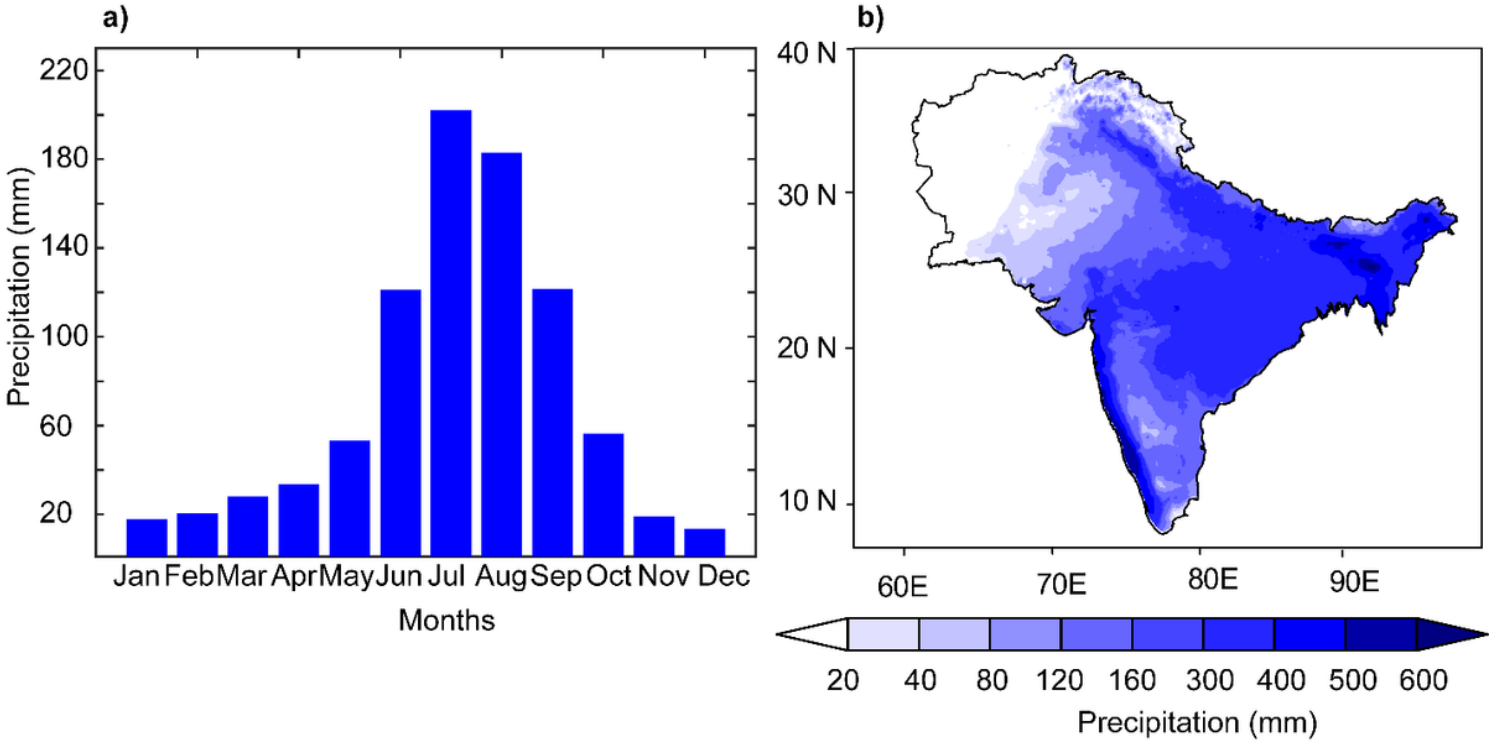

Figure 2

a) The climatology of area averaged monthly mean precipitation and b) The spatial pattern of monsoon precipitation during JJAS during 1988-2008. Note: The designations employed and the presentation of the material on this map do not imply the expression of any opinion whatsoever on the part of Research Square concerning the legal status of any country, territory, city or area or of its authorities, or concerning the delimitation of its frontiers or boundaries. This map has been provided by the authors.

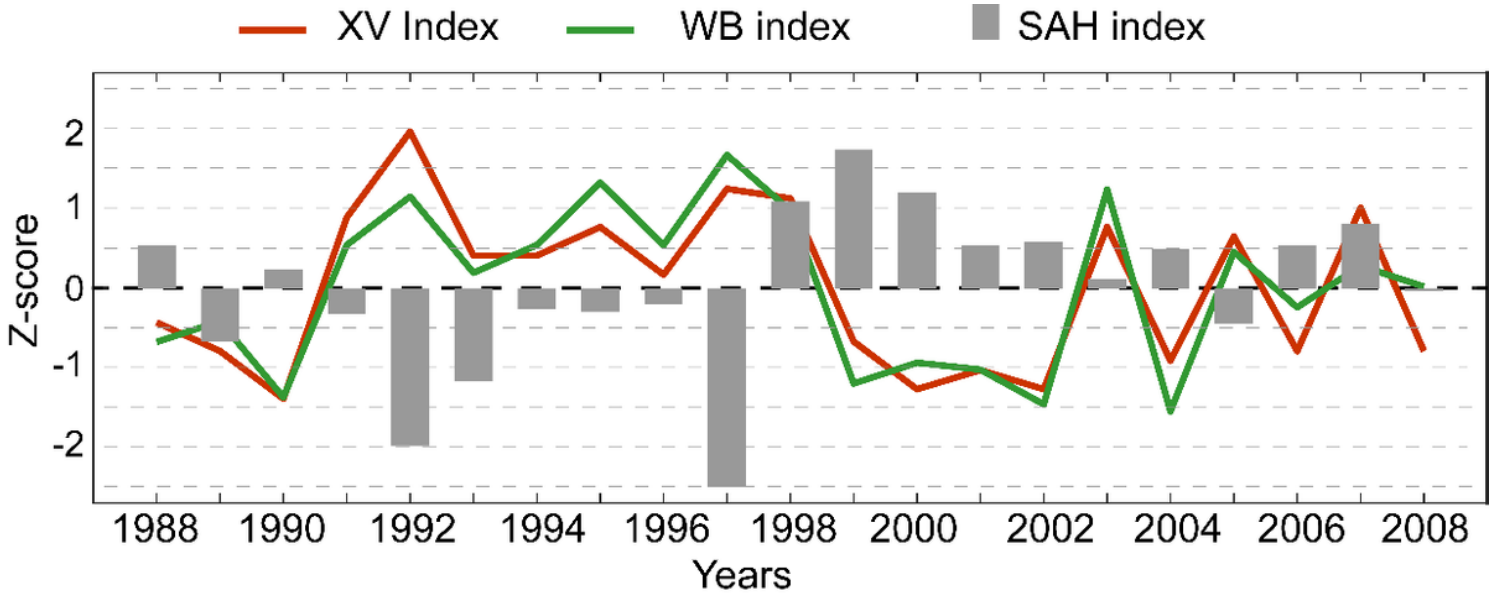

Figure 3

The standardized SAH index, the XV, and the WB monsoon onset indices during 1988-2008. The correlation field of the XV and WB index with SAH index is significant with a 95% confidence level.

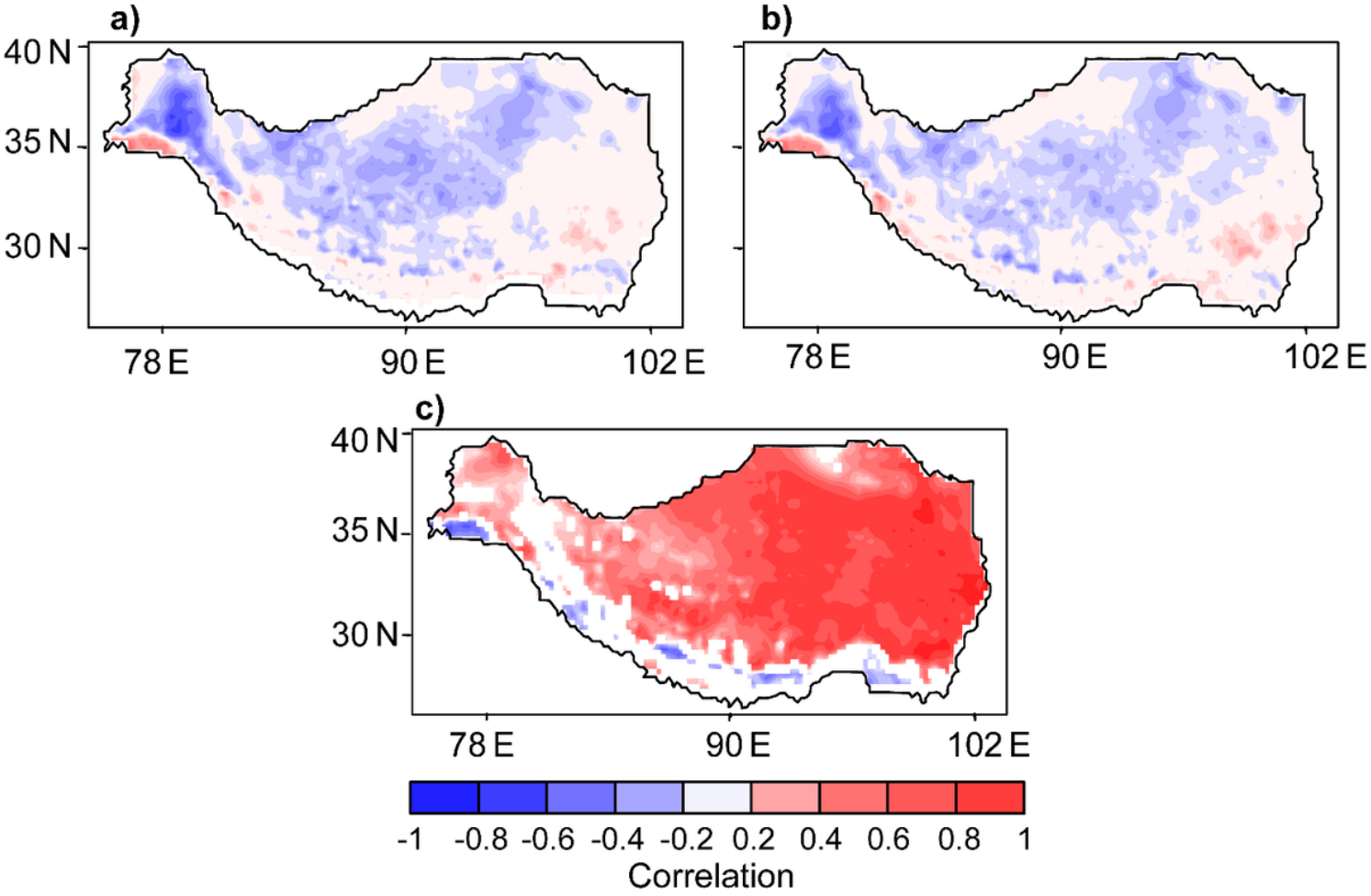

Figure 4

The pixel-wise correlation coefficients between spring TP soil moisture and each index during 1988-2008, a) the XV, b) the WB, and c) the SAH index. The shaded values have passed the significance test at a 5% level. Note: The designations employed and the presentation of the material on this map do not imply the expression of any opinion whatsoever on the part of Research Square concerning the legal status of any country, territory, city or area or of its authorities, or concerning the delimitation of its frontiers or boundaries. This map has been provided by the authors.

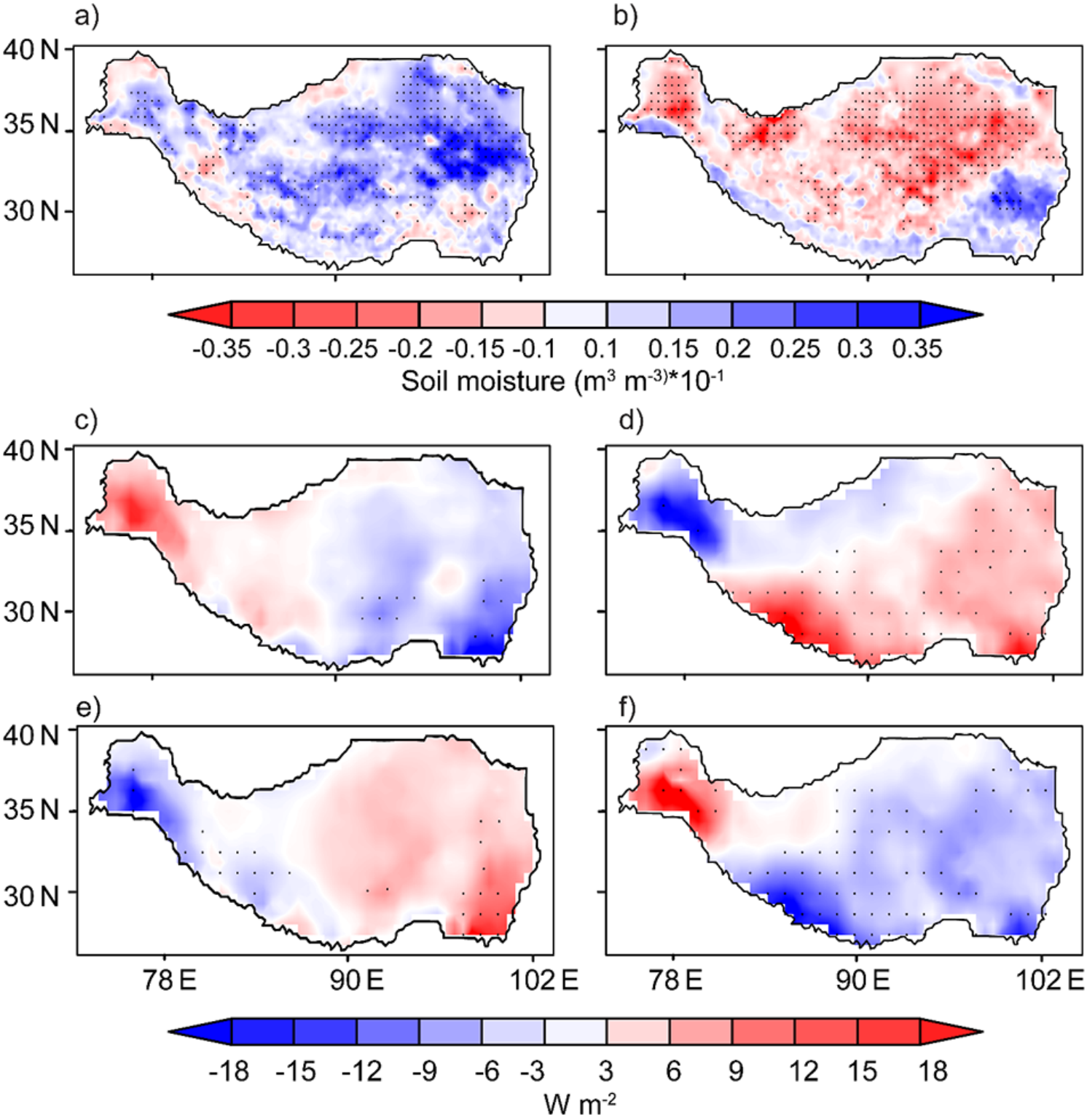

Figure 5

Soil moisture (a), sensible (c) and latent heat (e) composites in the early-onset composite, and those (b, d, f) in the late-onset composite, respectively. The stippling indicates a significant (95% confidence) difference in mean from the respective multiyear mean fields. Note: The designations employed and the presentation of the material on this map do not imply the expression of any opinion whatsoever on the part of Research Square concerning the legal status of any country, territory, city or area or of its

authorities, or concerning the delimitation of its frontiers or boundaries. This map has been provided by the authors.

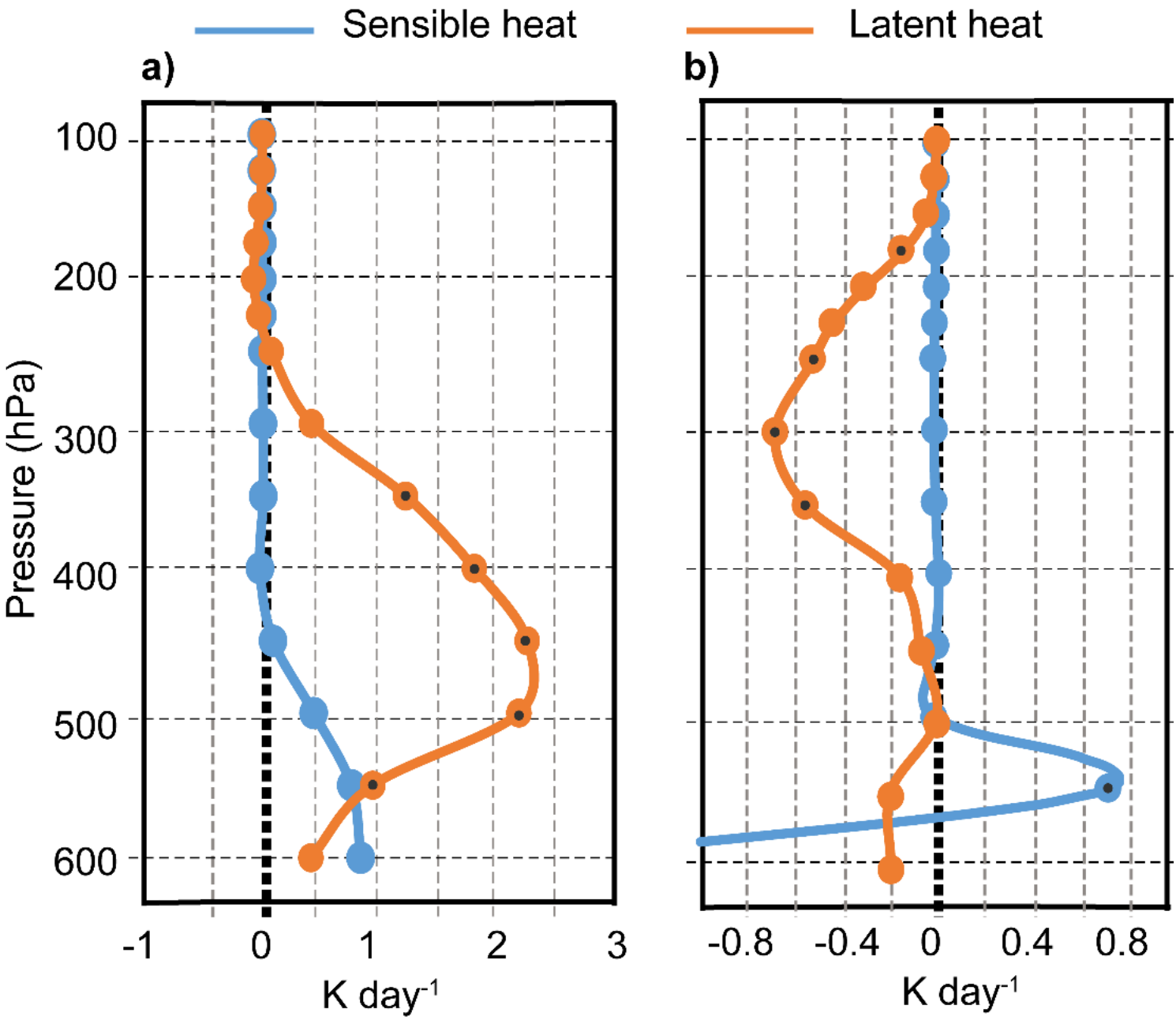

Figure 6

Vertical profiles of sensible and latent heat fluxes in spring of (a) early-, and (b) late-onset composites over TP. The heat fluxes are averaged within the area 26N to 37N and 85E to 103E. The black dots show a significant (95% confidence) difference in mean from the respective multiyear mean fields.

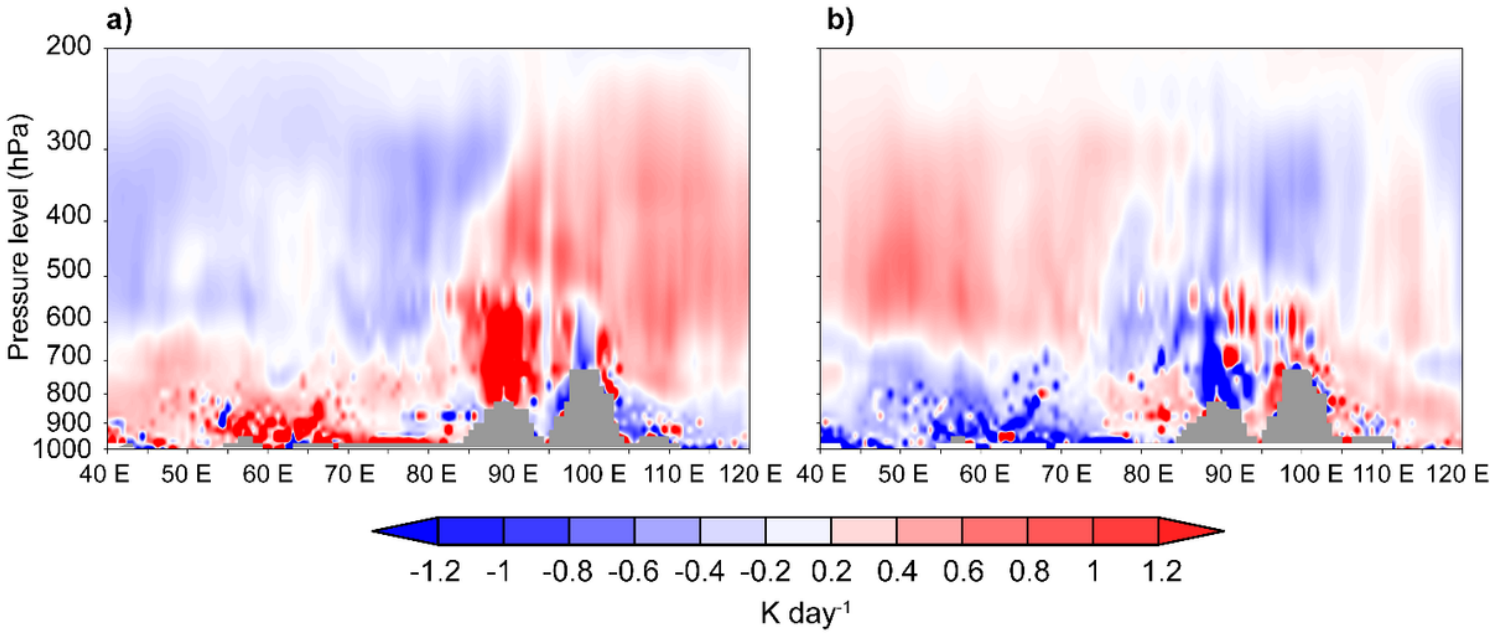

Figure 7

Vertical profiles of TP diabatic heating in (a) the early-onset, and (b) the late-onset years, which are averaged from 27N to 38N. Note: The designations employed and the presentation of the material on this map do not imply the expression of any opinion whatsoever on the part of Research Square concerning the legal status of any country, territory, city or area or of its authorities, or concerning the delimitation of its frontiers or boundaries. This map has been provided by the authors.

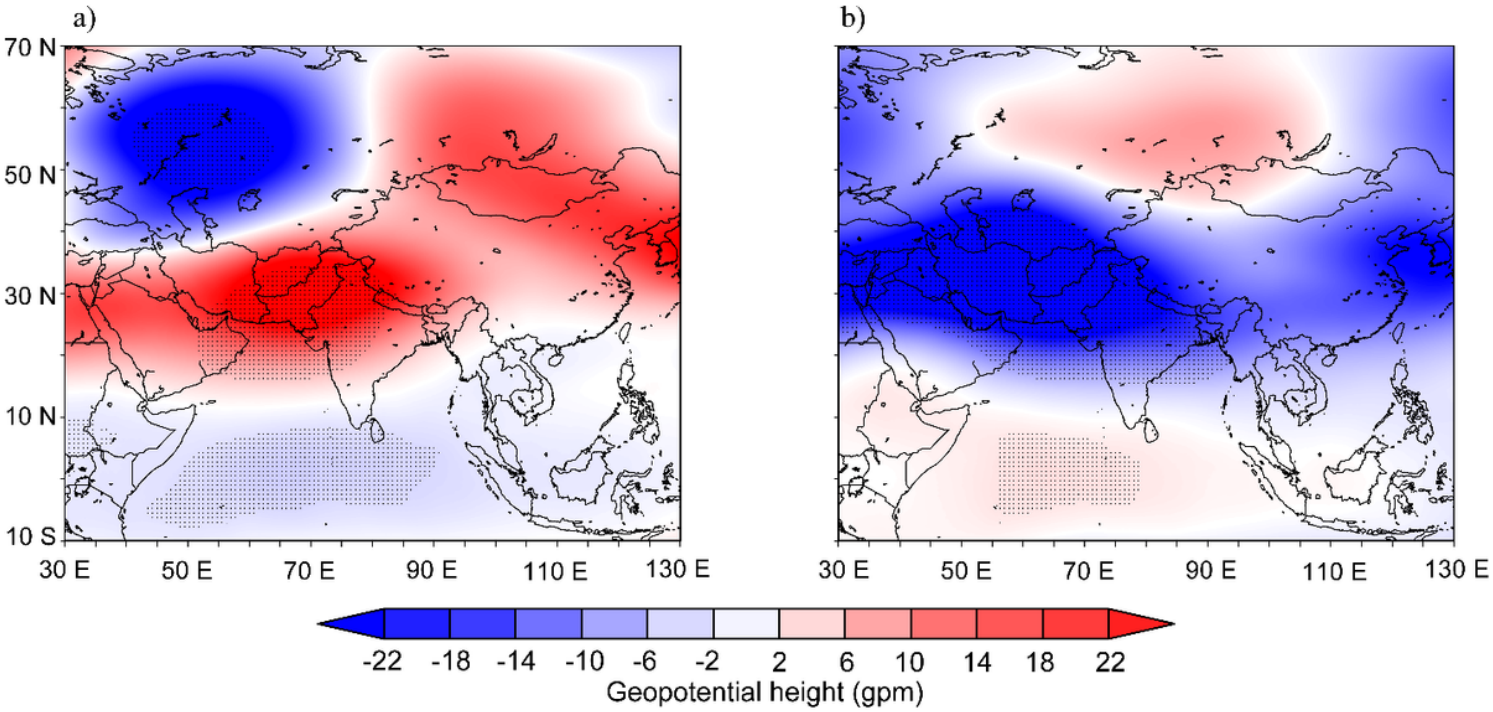

Figure 8

The South Asian High (SAH) anomalies at 200 hPa in spring of (a) the early-onset and (b) late-onset composites. The black dots show a significant (95% confidence) difference in mean from the respective multiyear daily mean fields. Note: The designations employed and the presentation of the material on this map do not imply the expression of any opinion whatsoever on the part of Research Square concerning the legal status of any country, territory, city or area or of its authorities, or concerning the delimitation of its frontiers or boundaries. This map has been provided by the authors.

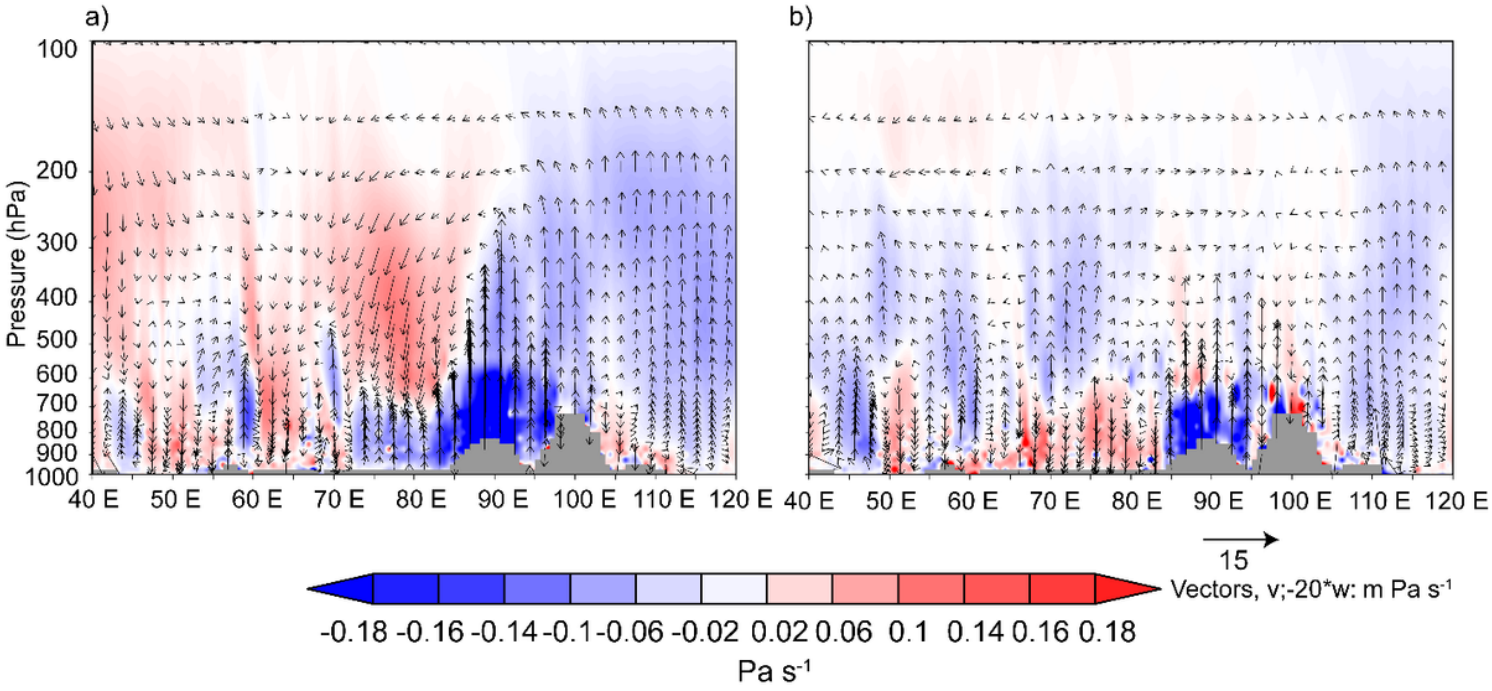

Figure 9

Latitudinal average of vertical velocity and meridional wind over TP in (a) early- and (b) late-onset composites. The latitudinal profiles are calculated for the area-average of (27N to 38N). The grey color shows the topography of the TP. Note: The designations employed and the presentation of the material on this map do not imply the expression of any opinion whatsoever on the part of Research Square concerning the legal status of any country, territory, city or area or of its authorities, or concerning the delimitation of its frontiers or boundaries. This map has been provided by the authors.

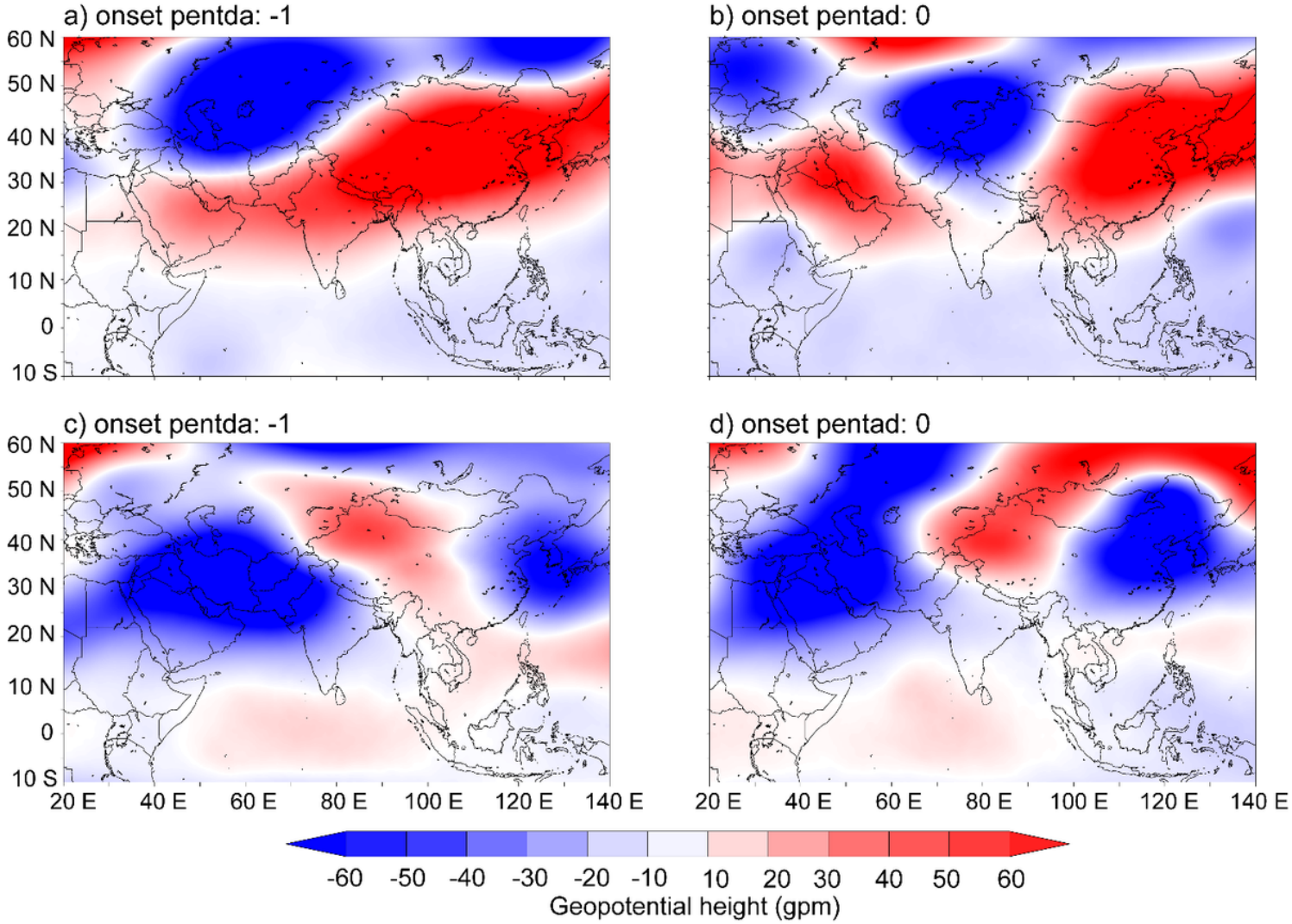

Figure 10

The SAH pentad anomalous evolution during early and late-onset composites. The a) onset pentad: -1 and b) onset pentad: 0 are for early-onset and c) onset pentad: -1 and d) late-onset: 0 are for late onset composites. Note: The designations employed and the presentation of the material on this map do not imply the expression of any opinion whatsoever on the part of Research Square concerning the legal status of any country, territory, city or area or of its authorities, or concerning the delimitation of its frontiers or boundaries. This map has been provided by the authors.

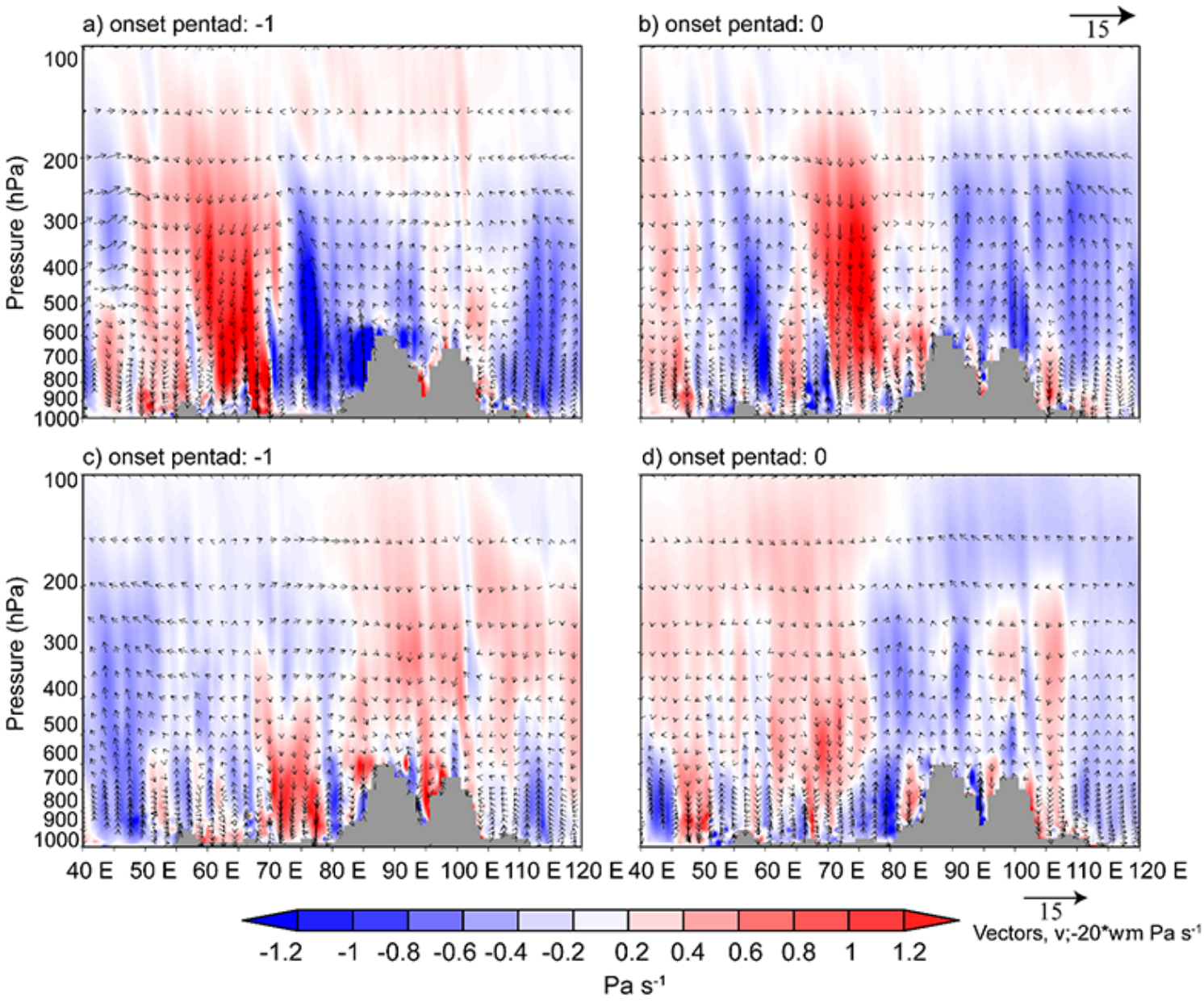

Figure 11

The meridional wind (vectors) and vertical velocity (shaded) pentad anomalies of the early and late-onset composites. The a) onset pentad: -1 and b) onset pentad: 0 are for early-onset, and c) onset pentad: -1 and d) late onset: 0 are for late onset composites. The latitudinal profiles are calculated for the area-average of (27N to 38N). Note: The designations employed and the presentation of the material on this map do not imply the expression of any opinion whatsoever on the part of Research Square concerning the legal status of any country, territory, city or area or of its authorities, or concerning the delimitation of its frontiers or boundaries. This map has been provided by the authors.

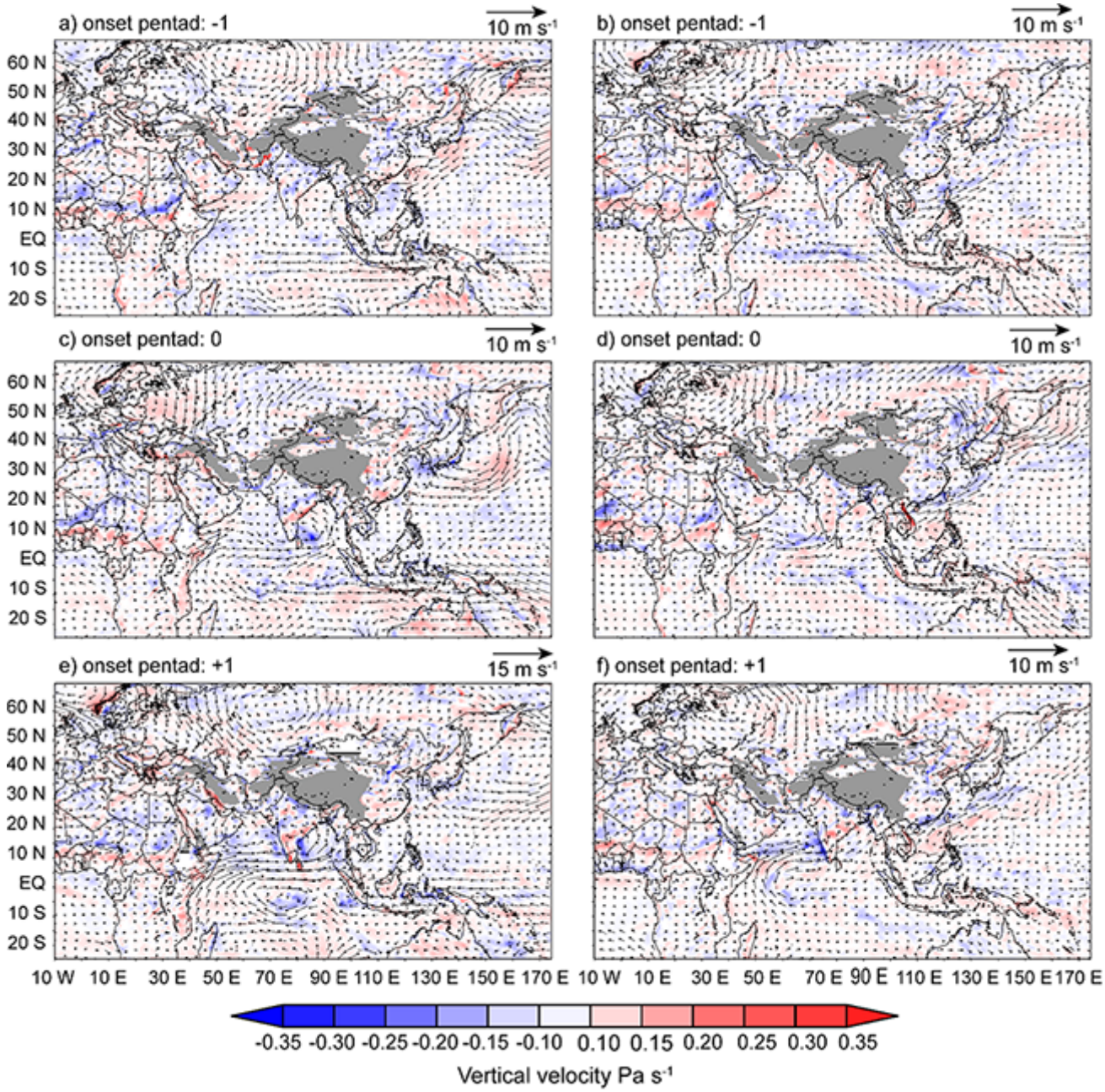

Figure 12

The wind components (vectors) and vertical velocity (shaded) pentad anomalies for early, and late-onset composites. The a) onset pentad: -1, b) onset pentad: 0 and c) onset pentad: +1 are for early-onset and c) onset pentad: -1, d) late-onset: 0 and c) onset pentad: +1 are for late onset composites. Note: The designations employed and the presentation of the material on this map do not imply the expression of any opinion whatsoever on the part of Research Square concerning the legal status of any country, territory, city or area or of its authorities, or concerning the delimitation of its frontiers or boundaries. This map has been provided by the authors.